Iceberg Stability Investigations Using Machine Learning for Alaska and Greenland

Sachiko Ka'ikilaniali'iopuna Sakai

Thesis submitted to the faculty of the Virginia Polytechnic Institute and State University
in partial fulfillment of the requirements for the degree of

Master of Science
In
Geosciences

Michael J. Willis, Chair
Christina Dura
Christopher L. Thomas

December 3, 2025
Blacksburg, Virginia

Keywords: cryosphere, iceberg capsize, natural hazard, machine learning

Iceberg Stability Investigations Using Machine Learning for Alaska and Greenland

Sachiko Ka'ikilaniali'iopuna Sakai

ABSTRACT

Iceberg-capsize tsunamigenesis is a coastal hazard not often discussed or observed due to the low frequency with which this process occurs. Greenlandic communities are proximal to coasts and are at risk of tsunamis caused by unprompted iceberg-capsize. We use time-lapse imagery from our own sites in Greenland (QORQ, UMNQ, NIAQ, INKF) accompanied with imagery from LeConte Glacier, Alaska field campaigns to identify and measure unstable (capsizing, fragmenting, disintegrating) icebergs and compare them to stable icebergs. While there are studies that investigate the mechanics of capsize, there are little to none which offer applicable results to implement in real-world scenarios for hazard mitigation. We use ground imagery to observe icebergs and investigate the probability of an iceberg being unstable based on its geometry. We also use air temperature collected from meteorological data from respective sites to compare with unstable event occurrences. We find that it is not likely there are implications that air temperature has an influence on iceberg stability for both Alaska and Greenland. For Alaska, we find that logistic regression models may be able to differentiate between stable and unstable icebergs. Model scores for Alaska data and respective sampling methods: no sampling (85.07%), RMU (65.10%), SMOTE (66.14%). For Greenland, we speculate the data set may be too small and generalizes most icebergs as stable and the logistic regression seemingly has more difficulty with classification: no sampling (79.16%), RMU (57.14%), SMOTE (80.10%).

Iceberg Stability Investigations Using Machine Learning for Alaska and Greenland

Sachiko Ka'ikilaniali'iopuna Sakai

GENERAL AUDIENCE ABSTRACT

When icebergs suddenly capsize or rollover, they can induce tsunamis. This motion describes iceberg-capsize tsunamigenesis which is a coastal hazard that is not often discussed and rarely observed. Communities in Greenland, which are in proximity to coasts, are at risk of potential tsunami sources. There are few studies which offer applicable results to implement in real-world scenarios for iceberg hazard mitigation. We investigate with ground imagery to observe icebergs and use machine learning to classify the probability of an iceberg being unstable. We use time-lapse imagery from LeConte Glacier, Alaska and our own sites in Greenland to identify and measure unstable icebergs and compare them to stable icebergs. We also use air temperature from respective sites to compare with unstable event occurrences. We find it is not likely there are implications that air temperature has an influence on iceberg stability in both Alaska and Greenland. We also find that the Alaska models may show potential to be able to differentiate between stable and unstable icebergs. In contrast, the Greenland models appear to not be able to distinguish stable and unstable icebergs.

Acknowledgements

I would like to thank my advisor, Mike Willis, for encouragement and patience while working on this project. I would also like to thank my committee members, Tina Dura and Chris Thomas, for their advice and encouragement as well. I also extend gratitude to our colleagues at ASIAQ for assisting in fieldwork and installing the cameras. I am glad I was able to meet my lab members Maria De Los Santos, Jarely Mendez, and Fernanda Gastelu through this experience. Grad school would not have nearly been as fun. My partner, family, and friends also provided tremendous amounts of support, and I am deeply grateful for that.

Funding for this work was provided by Navigating New Arctic National Science Foundation Greenland Hazards Project.

Table of Contents

List of Figures

List of Tables

1. Introduction

1.1 The Greenland Ice Sheet and its Associated Coastal Hazards

The cryosphere consists of places on Earth characterized by the presence of snow and ice. Structures like ice sheets and ice caps have remained frozen since the Last Glacial Maximum, about 20,000 years ago, and hold significant amounts of water (Bloch et al., 2013, Sherriff-Tadano et al., 2024). Greenland's (Kalaallit Nunaat) interior is covered by the largest ice sheet in the Arctic, and its changes are studied extensively to understand climate changes' current and future impacts (Figure 1) (NSIDC, 2025).

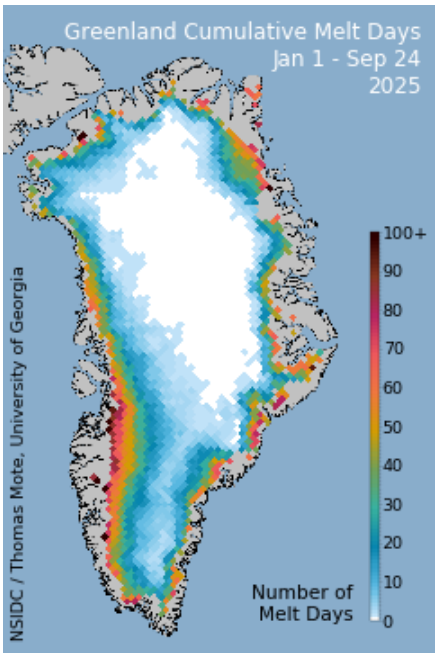

Figure 1. NSIDC maps of Greenland Ice Sheet of cumulative melt days from 1/1/2025 through 9/24/2025 (Mote, 2025)

The Greenland Ice Sheet (GrIS), "Sermersuaq – the great ice" in Greenlandic, is the second largest contributor to global sea level rise (SLR), after thermal expansion (Shepherd et al., 2012, Zemp et al., 2019, Bollen et al., 2023, Poinar et al., 2023) and is the top contributor of barystatic sea level rise (Hofer et al., 2020). The predicted contribution of the total volume of freshwater within the GrIS equates to approximately

7.4 meters of global sea level rise (Morlighem et al., 2017) and it could provide a total of up to 33 millimeters of SLR by the year 2100 (Aschwanden et al., 2019, Nias et al., 2023). Observing the mass and surface elevation of the GrIS with gravimetry and altimetry is important because ice is sensitive to changing temperatures and is used as an indicator of current and future climate conditions (Bloch et al., 2013, Fahrner et al., 2021, Minor et al., 2023 Bollen et al., 2023, Berg et al., 2024).

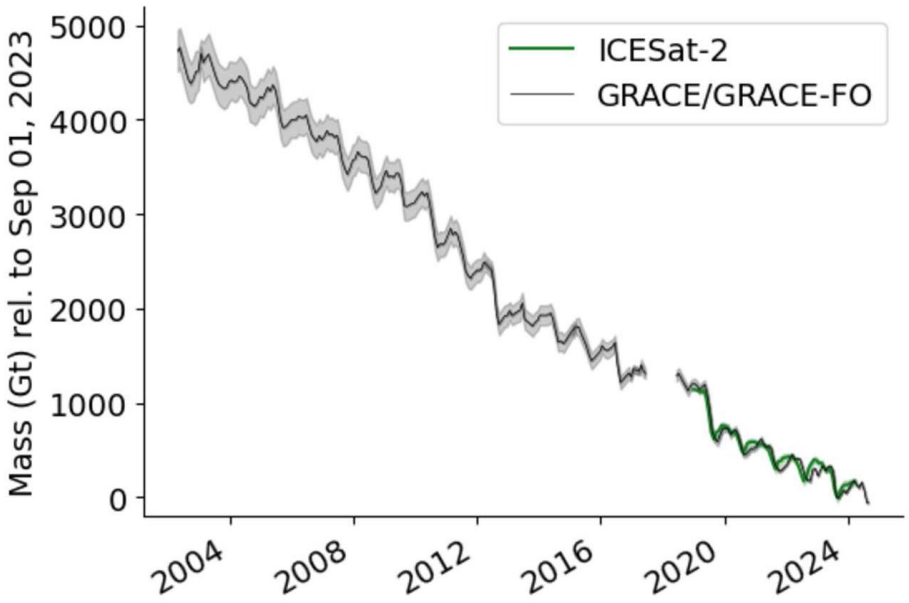

Figure 2. From NOAA's Arctic Report Card for the Greenland Ice Sheet (Poinar et al., 2024). GRACE/GRACE-FO (black line) and ICESat-2 (green line) observations of the Greenland Ice Sheet mass balance from 2002 to 2024. Uncertainties are shaded in light gray.

Since the mid-1990s the GrIS has shown an overall increasing trend of ice mass loss in both surface mass balance (SMB) and dynamic mass change (Poinar et al., 2023, Bollen et al., 2023, Kc et al., 2025). SMB describes the variance between glacier surface

accumulation and meltwater runoff. Dynamic mass loss encompasses multiple processes including terminus retreat, crevassing, glacial calving, and ice flow (Figure 3).

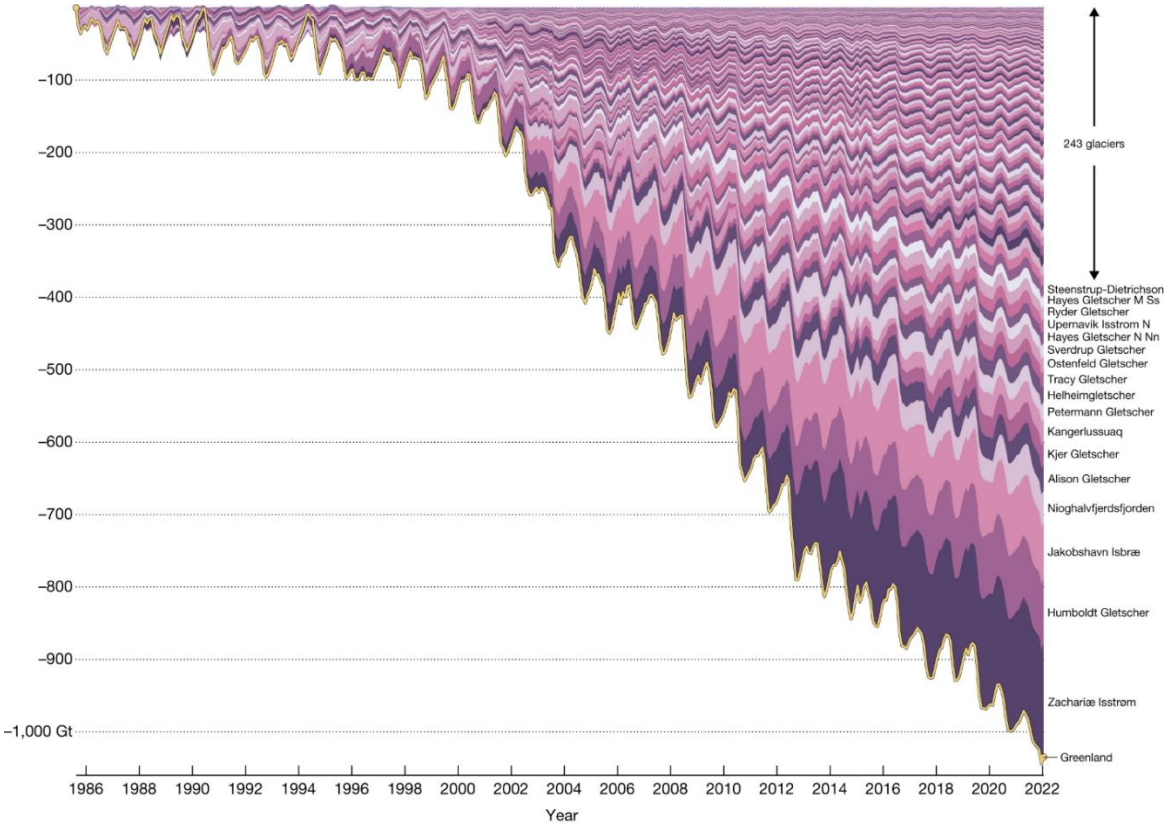

Figure 3. Cumulative mass change from Greenland glaciers from 1986 until 2022 (Greene et al., 2024)

There are ongoing discussions on whether SMB or dynamic mass change is leading overall in mass loss, however we focus on dynamic mass loss. Work from Greene et al. (2024) states that studies neglecting calving front-retreat in their dynamic mass loss calculations means Greenland's total mass loss could be underestimated up to 20%. Kc et al. (2025) brings attention to seasonal terminus ablation (retreat and advance) and ice flux's significant impact on total ice mass which is generally included in discharge measurements. They find these combined processes to cause an underestimation on total GrIS mass loss of approximately 14 Gt yr^{-1}. The processes of dynamic mass loss are

normal and are the mechanism by which glaciers maintain their equilibrium during seasonal changes. However, the concern is that there is an acceleration and increase in magnitude of dynamic mass losses. Additionally, upstream fjord dynamics' influence on glaciers' movement and rate of change are not fully understood. There remains uncertainty about how dynamic mass loss will affect Greenland in the future.

Figure 4. Nuuk, Greenland

All Greenlandic communities are coastal (Figure 4) as the GrIS covers approximately 80% of the interior of the country. Therefore, marine access is integral for Greenlander's lifestyle for fishing, trade, and transportation between towns. The rapidly changing landscape is of increasing concern for some people within these communities (Minor et al., 2023). Coastal hazards that Greenlandic communities encounter that are influenced by ice and dynamic mass loss include mass movements (landslides), landslide generated tsunamis, coastal inundation, coastal erosion, debris flow and iceberg hazards (Fritz et al., 2017, Minor et al., 2019). Tsunamis have had significant impacts in

Greenland. The Karrat Isfjord tsunami on June 17th, 2017, impacted the town of Nuugaatsiaq (32 km away from the landslide) where runup of 9 meters resulted in damaged and destroyed infrastructure, several injuries and four fatalities (Figure 5) (Strzelecki and Jaskolski, 2020). Another landslide tsunami in remote East Greenland on September 16th, 2023, had a maximum height of 200 meters and produced enough energy to sustain a seismic signal lasting 9 days (Figure 5) (Paddison 2024, Svennevig et al., 2024).

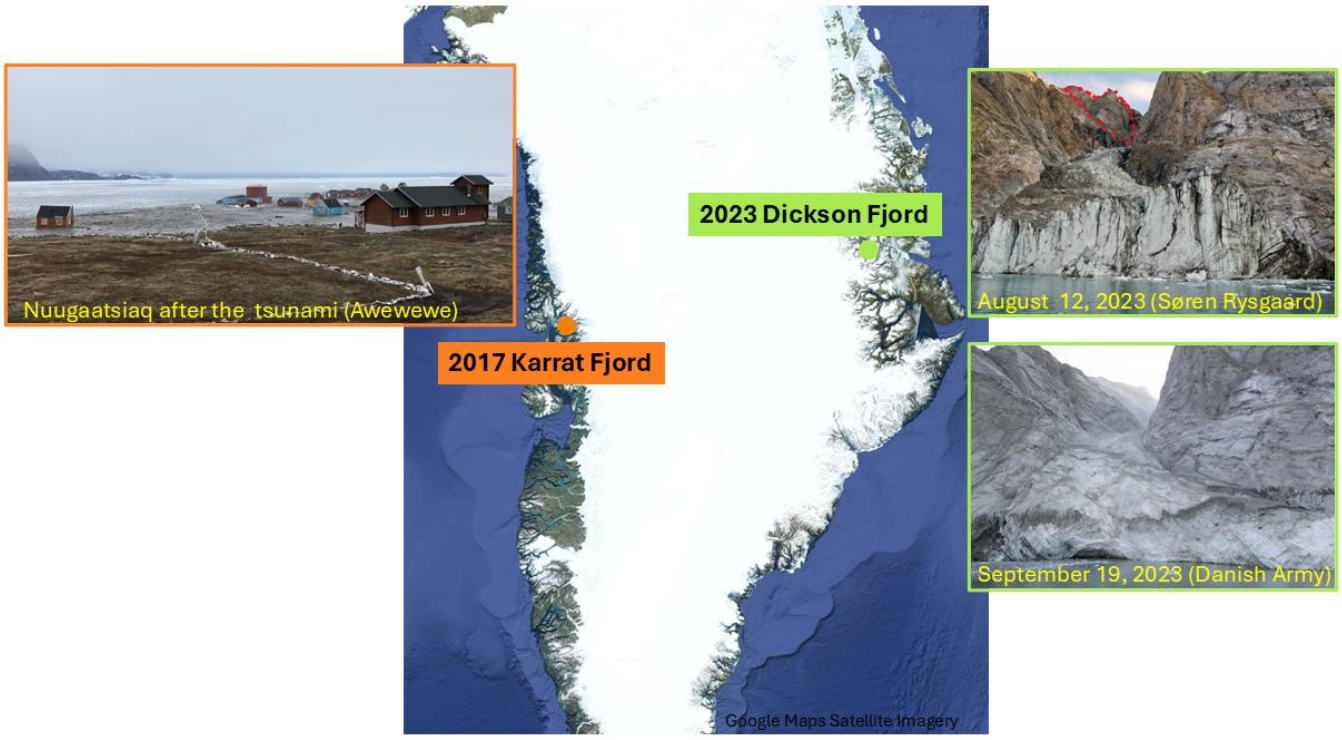

Figure 5. Map of Greenland showing 2017 and 2023 tsunami locations

Natural hazards in Greenland are predicted to become more prevalent due to the rapidly changing climate's impact on ice mass loss (Long et al., 2015, Sugiyama et al., 2021, Chudley et al., 2025). Accelerating glacier calving rates also increases the concern about iceberg hazards to Greenlandic communities (Bollen et al., 2023).

Icebergs are pieces of ice that have dislodged from the face of a glacier (terminus) into open waters. Iceberg capsize (or iceberg rollover) is a hazard created from the sudden movement of an iceberg sinking or rolling over and disturbing the surface of the water. In cases where an iceberg is large enough to induce a tsunami, the event is called iceberg capsize tsunamigenesis (MacAyeal et al., 2011). Based on the impact tsunamis have had in Greenland and comments from Greenlanders, studying a potential tsunami source such as capsizing icebergs is important (Burton et al., 2012, Long et al., 2015, Svennevig 2019, Heller et al., 2021, Wolper et al., 2021).

1.2 Using Machine Learning for Cryosphere Hazards

Computer vision is well-established and a rapidly developing field in artificial intelligence that uses machine learning models to extract information from imagery or videos to generate predictions. Cryosphere studies often utilize segmentation to study ice features with remote sensing including glaciers, glacier lakes, permafrost, sea ice, icebergs and others (Shankar et al., 2024). Segmentation is a task within computer vision that has the goal of dividing an image into groups of pixels based on specified criteria. We attempted to utilize segmentation to derive iceberg measurements, however we faced issues with distinguishing between water and icebergs. While segmentation can be useful in a future study, we use manual measurements for this study.

The utilization of satellite imagery for cryosphere studies can be attributed to spatial resolution, spatial extent, reliable temporal coverage, and cost efficiency (Osco et al., 2023, Ye et al., 2024). Iceberg tracking projects commonly use spaceborne radar data because the difference in backscatter between water and an iceberg is distinctive and data collection can occur at night and in cloudy conditions. Studies using semi-supervised

algorithms for segmenting icebergs have contributed to studies focused on iceberg size-distributions and sea ice maps. Scheick et al. (2019) use segmentation to remove cloud cover in optical imagery, assist with differentiating icebergs from water and collecting the size of icebergs. Koo et al. (2023) uses a simple segmentation to identify icebergs and then later applies an advanced segmentation to obtain accurate iceberg shapes.

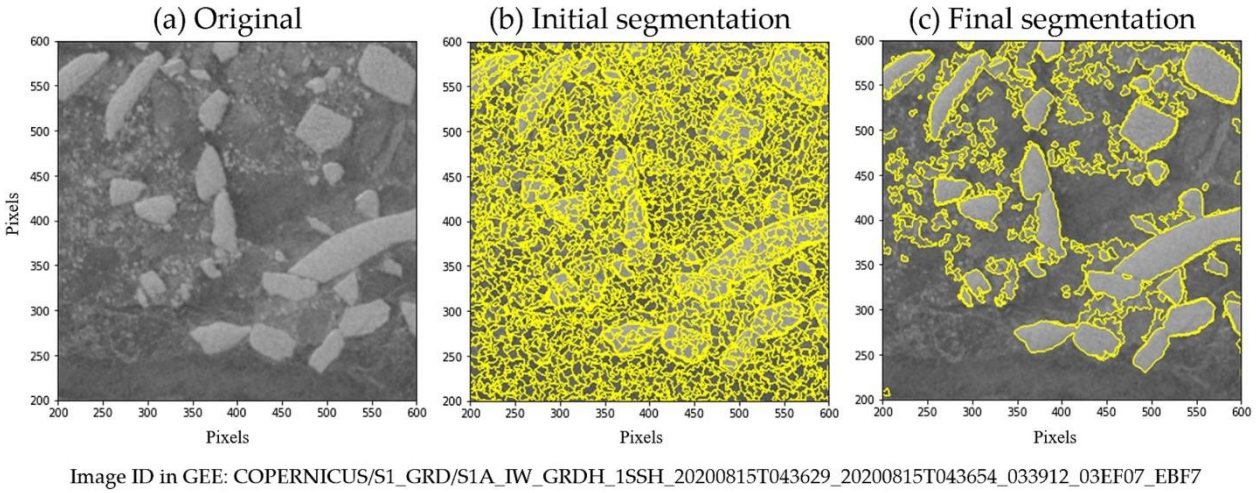

Figure 6. Example of iceberg segmentation for remote sensing data from Koo et al. (2023)

However, satellites only provide a top-down perspective for icebergs, and their temporal resolution cannot capture capsize events which can occur in minutes. This study uses ground-based imagery that provides a side-view perspective and high temporal resolution, allowing us to identify capsize events. Some drawbacks to using ground imagery include the fixed location and lack of mobility and camera distortion with an increase in distance away from the camera. A developing application of ground imagery is the goal of assisting ships and vessels in avoiding collision with icebergs and sea ice (Kim et al., 2019, Ding et al., 2023).

1.3 Scope of the Study

1.3.1 The Importance of Iceberg Hazard Studies

Iceberg capsize is a natural hazard within the polar regions and is anticipated to become an increasing concern in the future (Long et al., 2015). Climate change is accelerating rates of glacial calving, contributing to the generation of icebergs (Scheick et al., 2019, Greene et al.,2024). Iceberg capsize can have destructive impacts on infrastructure and lives (MacAyeal et al., 2011, Heller et al., 2019). Towns situated near productive glaciers outlets have the potential to experience waves generated by icebergs (Normandeau et al., 2021). Some Greenlanders have experienced their boats being run aground along the rocky shoreline by waves which can damage or destroy their boats, which in turn affects their ability to travel and fish and hunt, affecting their income. Marc Buriot, an Uummannaq resident stated, "While we think about (landslide generated) tsunami, we really worry more about icebergs causing the big waves that can damage our boats" (*Personal Communication* 2023). Heidinnguaq Jensen, another resident of Uummannaq, told us of a concerning, small tsunami that was in the harbor there in July 2025 (*Personal Communication*, 2025).

1.3.2 Motivation, Goal, and Objectives

This study is motivated by the exploration of the probability of iceberg capsize occurring. The goal is to be able to predict the probability of risk of an iceberg being unstable based on its measurements and time of occurrence.

Objectives for this study are listed below:

- Compile a dataset containing measurements of icebergs with labels based on stability
- Determine iceberg population characteristics for sites in Greenland and Alaska

- Train, test and evaluate a machine learning model on the curated dataset to predict the probability of an iceberg being unstable
- Explore the relationships between internal iceberg measurements, event timing, and iceberg stability

1.3.3 Questions and Hypotheses

Questions:

- What is the relationship between an iceberg's geometry (width, height, aspect ratio) and its stability?
- Is there any influence of environmental conditions that promote capsize?

Hypotheses:

- I hypothesize that iceberg geometry (width, height) will provide information that can be used to predict whether an iceberg is stable or if it is likely to capsize, disintegrate, or fragment.
- I hypothesize there will be a difference between populations of stable and unstable icebergs.

2. Background

2.1 Positioning of Current Work

MacAyeal et al.'s (2011) study into iceberg tsunami hazards brought attention to iceberg capsize as a natural hazard and declared that the majority of capsize events occur within icebergs' early stages of formation. Capsize and fragmentation can occur when icebergs readjust their mass to their environmental conditions. They also investigated iceberg thickness in relation to generated tsunami heights (Figure 7).

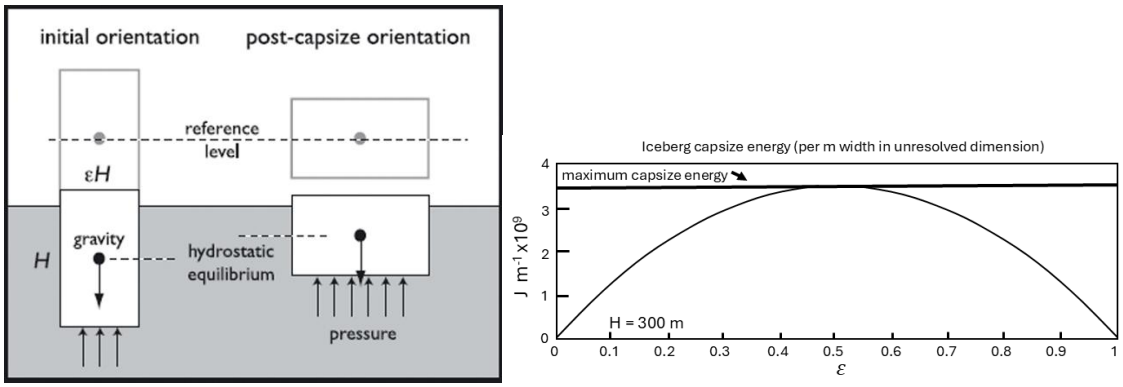

Figure 7. Diagrams from MacAyeal et al. (2011) showing basic iceberg capsize mechanics (left) and energy released by iceberg capsize (right)

Further studies into capsize mechanisms used simulations of controlled environments and theoretical numerical modelling methods to analyze the generation of waves from capsize. Burton et al. (2012) uses an acrylic water tank with tabular icebergs represented by rectangular low-density plastic. From there they modeled iceberg stability at different degrees of rotation against icebergs' aspect ratio (Figure 8).

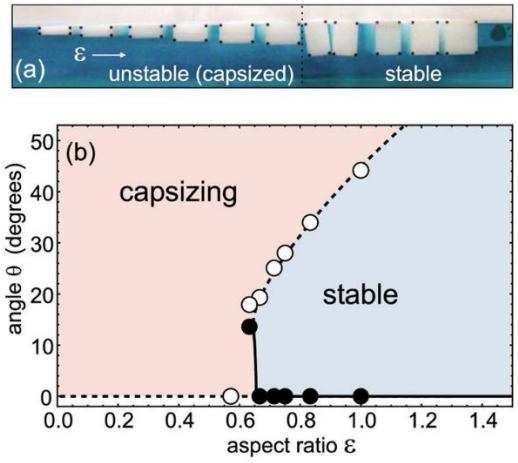

Figure 8. Results from Burton et al. (2012) showing boundary between stable and unstable icebergs based on their aspect ratio

Their results show that when an iceberg's aspect ratio surpasses a critical ratio, Ɛ, it becomes unstable. There can also be cases where the aspect ratio is small, but an

external force is able to propagate the iceberg over the unstable threshold. Wagner et al.'s (2017) study follows up on Burton et al. (2012) by using the critical ratio for rolling tabular icebergs to further improve the accuracy of existing numerical models. Heller et al. (2019) conducted large scale experiments in 50m x 50m water tanks to observe the magnitudes of energy released by capsizing and different types of calving icebergs. Bonnet et al. (2020) used computational fluid dynamics and semi-analytical simplified fluid-structure model (SAFIM) in an effort to determine the accuracy of simulated capsize. Results proved that SAFIM produces accurate results compared to other models, however there is 5-25% error in simulations depending on the iceberg aspect ratios. Hester et al. (2021) found that iceberg aspect ratio influences iceberg melting rates and icebergs with smaller aspect ratios with non-uniformities are predicted to have increased melting rates.

Studies using field data are sparce but also significant. Long et al. (2015) used sedimentological tsunami deposits from a coastal lake to provide evidence of an iceberg induced tsunami that occurred ~6,000 years ago in Innaarsuit (Northwest Greenland), Disko Bay with 3.3 meters minimum of runup height. Predictions that iceberg tsunamis are more prevalent near marine-terminating glaciers are also noted (Long et al., 2015). In Antarctica Ke et al. (2022) used time-series to attempt to predict iceberg induced tsunamis occurring near Dålk Glacier.

Learning about the mechanics of capsize is important and these studies are useful for determining the physics of capsizing in controlled environments. However, observations of real situations are more complex. An example of this is that the critical ratio can't truly be applied in the field because most of an iceberg is obscured by water.

While an estimate of iceberg depth can be calculated from density (assuming uniform density), the exact shape would remain unknown. This work attempts to provide a practical, operational way to identify unstable icebergs that can be applied towards hazard mitigation in Greenland.

Figure 9. July 8th, 2025, iceberg threatening coastal town (Dennis Lehtonen)

Large icebergs threatening towns also make their way into news articles. In 2012, a tsunami generated by an iceberg was reported in Ilulissat Isfjord which almost destroyed the boat that captured the event (BBC News, 2012). In July 2018, Innaarsuit, the same town associated with Long et al.'s (2015) study on increasing iceberg hazards, had a 90-meter-tall iceberg stopped within the bay. The iceberg was stationary for weeks and there was fear it would capsize and cause a localized tsunami, but thankfully it drifted away without incident (The Weather Channel 2018, European Space Agency 2018, Time 2018, NASA Earth Observatory 2018). In July 2025 a large iceberg grounded

a second time at Innaarsuit and remained stationary for weeks. The iceberg ended up splitting into 2 large icebergs that again moved away without incident (Figure 9) (New York Post 2025, National Post 2025).

Iceberg capsize is a rarely occurring event which makes it difficult to study. We aim to understand if there are conditions where iceberg capsize is more likely to occur.

2.2 Physical Properties of Icebergs

Icebergs are produced by calving glaciers when ice separates from a glacier into a marine or lacustrine environment. To help identify and observe iceberg geometry, nomenclature for icebergs was created by the International Ice Patrol (IIP) and the World Meteorological Organization (WMO). There are 7 types of icebergs: tabular, non-tabular, blocky, domed, wedged, drydock, and pinnacle. There are also names to classify icebergs by their size, which in order from smallest to largest are: growler, bergy bit, small, medium, large and very large (Table 1).

Table 1. Table of iceberg classification based on measurements from International Ice Patrol

Category	Height (m)	Length (m)
Growler	< 1	< 5
Bergy bit	1 to 4	5 To 14
Small berg	5 to 15	15 to 60
Medium berg	16 to 45	61 to 122
Large berg	46 to 75	123 to 204
Very large berg	> 75	> 204

An iceberg's stability is influenced by its' geometry, which combined with gravity and buoyancy may force the iceberg to capsize, fragment or disintegrate (MacAyeal et al., 2011). Glaciological aspects of the source glacier and its calving style and environment determines an icebergs initial size and shape. The density of ice (~920 kg/m^3) is less than

freshwater (1000 kg/m^3) and saltwater (1025 kg/m^3) which causes icebergs to float (Sulak et al., 2017). The visible portion of an iceberg ranges from 9-11% of the total mass which is based on the buoyancy force of the ice within the body of water. Icebergs can have non-uniform densities and varying salinity compositions. Melting icebergs influence hydrodynamic processes due to their ability to influence currents, salinity and the amount and type of nutrients and minerals that they release into the water column (FitzMaurice et al., 2017).

2.3 Study Areas

2.3.1 Greenland

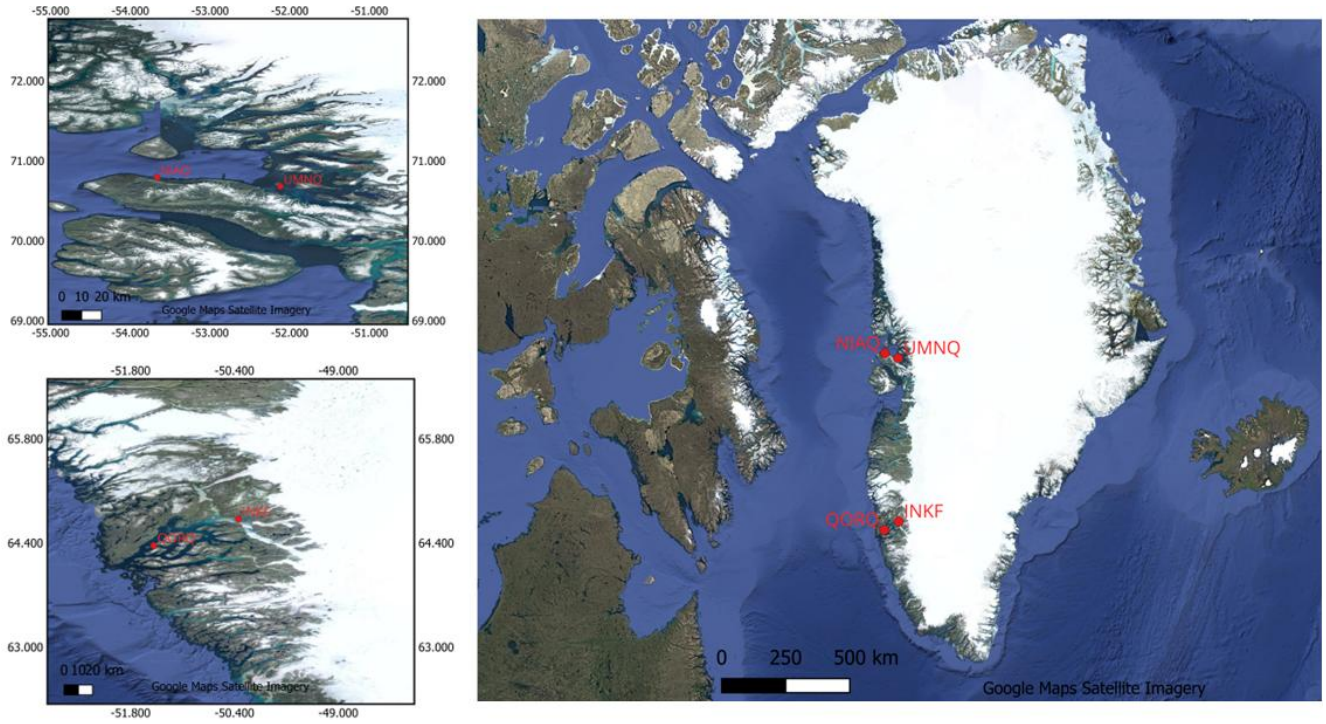

Figure 10. Map of Greenland site locations NIAQ, UMNQ, QORQ and INKF

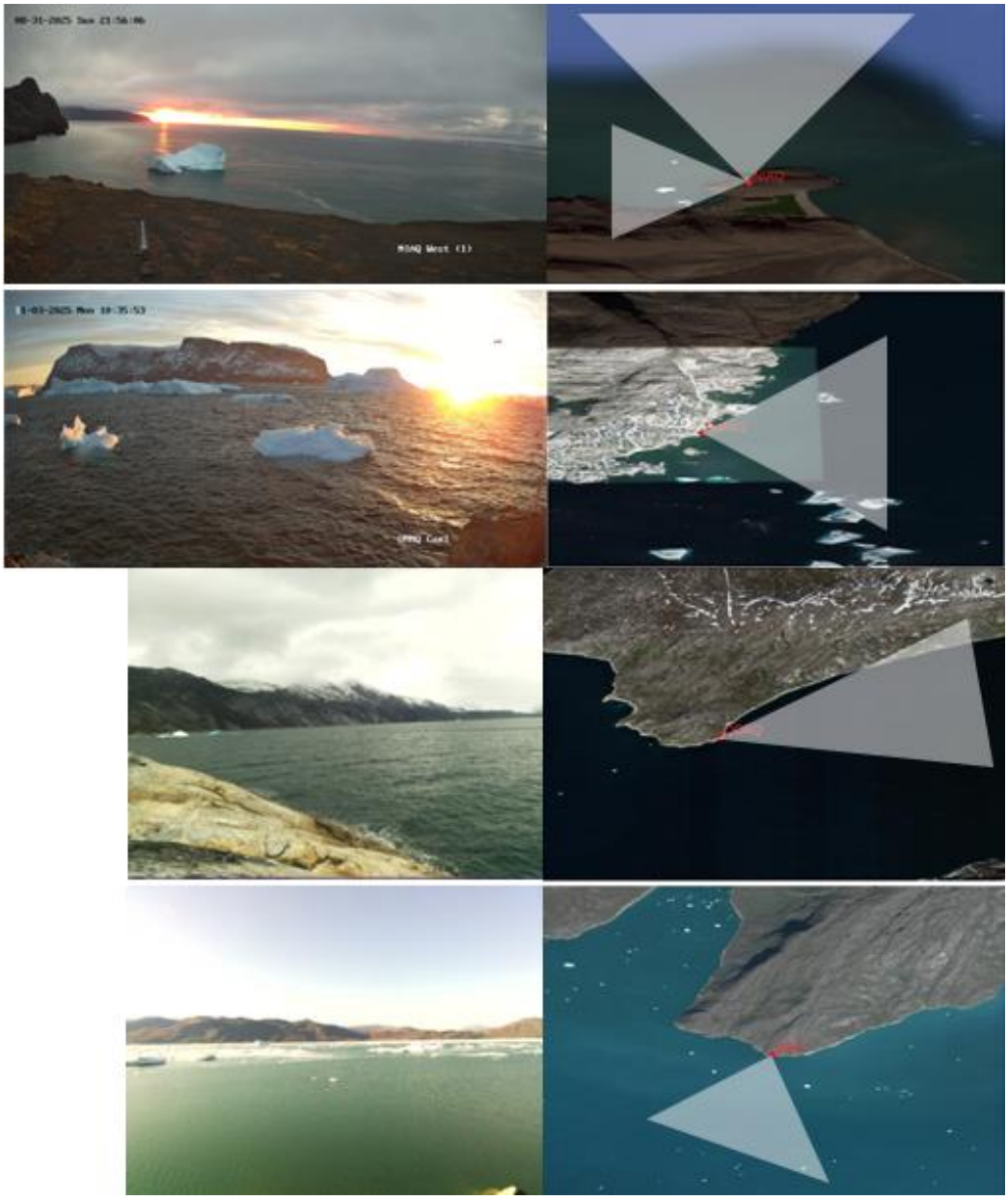

Figure 11. Fields of view for sites (from top to bottom) NIAQ, UMNQ, QORQ, INKF

Study sites were deployed in different locations along West Greenland in different fjord outlets to capture images of icebergs (Figure 10 and Figure 11). Uummannaq Fjord has sites NIAQ (70.792 N, 53.662 W), UMNQ (70.677 N, 52.115 W) and UPI0 (70.679 N, 52.115 W) and predominantly sees large icebergs produced from marine-terminating glaciers Store Glacier (*Qarassap Sermia*) and Lille Glacier (Sulak et al.,2017). NIAQ

occasionally sees large icebergs sourced from Jacobshaven glacier (Sermeq Kujalleq) far to the south, that have drifted around Disko Bay and the Nussuaq Peninsula. Nuuk Kangerlua fjord system has sites INKF (64.718 N, 50.343 W) and QORQ (64.362 N, 51.487 W) and icebergs are produced from Narsap Sermia and Kangilinngutaa Sermia. Icebergs observed at these sites appear in a variety of shapes including tabular, drydock, wedged and pinnacle. Iceberg sizes range from growlers to medium and occasionally large.

2.3.2 Alaska

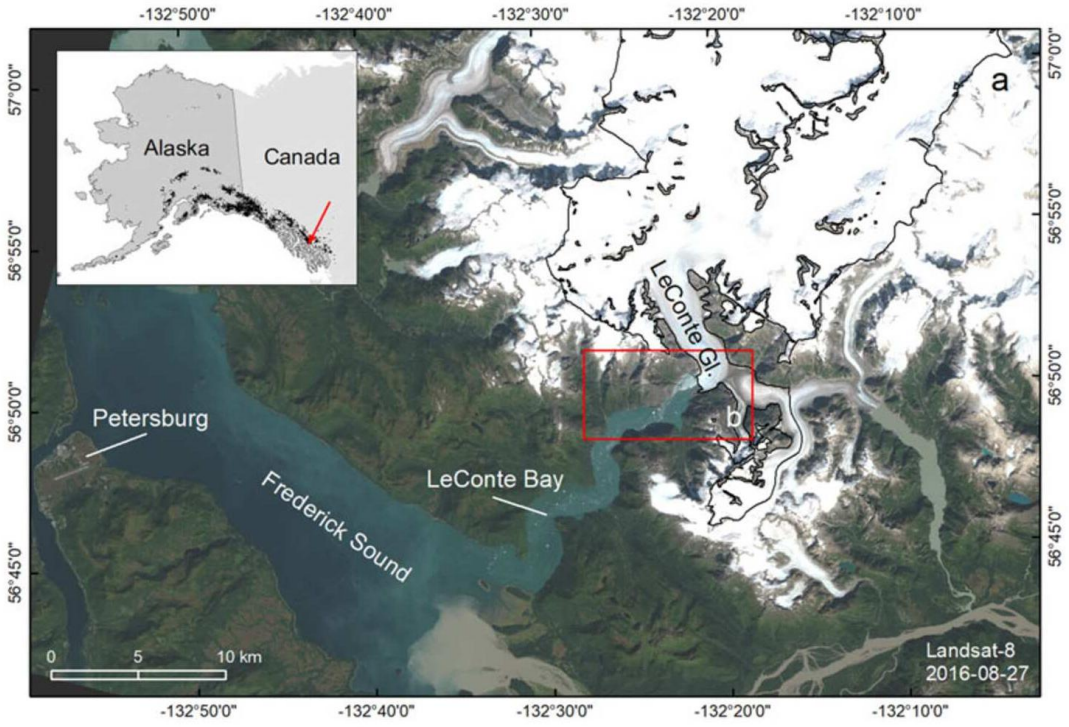

Figure 12. Map of LeConte Glacier (Landsat-8 imagery) from Kienholz et al. (2019)

LeConte Glacier in Southeast Alaska (Figure 12) feeds into the LeConte Bay (56.82 N, 132.39 W) and has been studied extensively because of its reputation as being one of the fastest melting glacier in Alaska (Abib et al., 2023). Data deposited in the NSF Arctic Data Center (arcticdata.io) was collected from multiple field campaigns from Amundson et al. (2017) (DOI 10.18739/A2J38KJ1W) and University of Alaska

Southeast (2020) (DOI 10.18739/A27W6754N). Both setups had multiple cameras and were stationed on the edge of the fjord overlooking the bay Figure 13. Solar panels were used to recharge the camera batteries. Each survey faced some technical problems when cameras would stop recording, as well as expected weather conditions like fog, rain, or snow obscuring the bay. Icebergs observed at these sites range from small to large, and occasionally very large. Most of the iceberg shapes include wedged, drydock, tabular, and non-tabular.

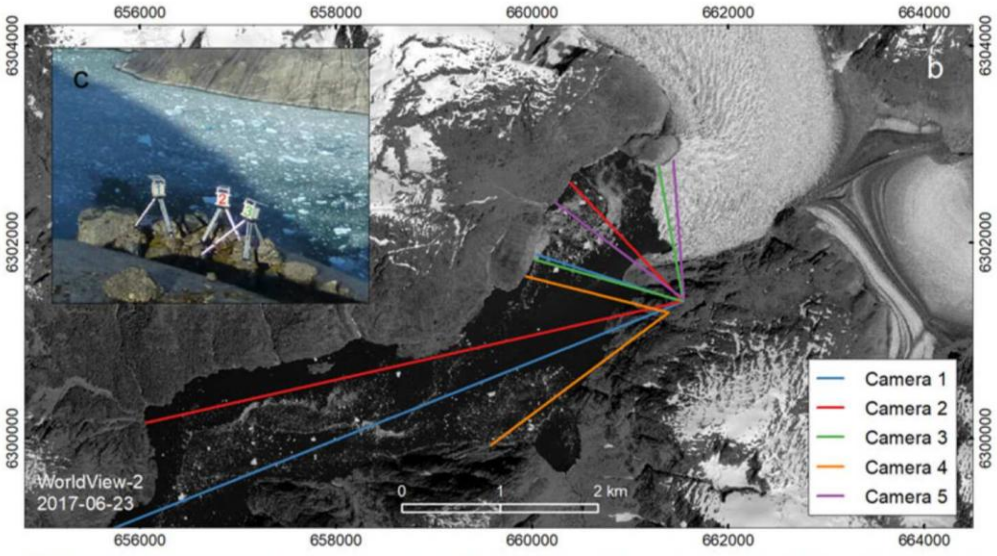

Figure 13. Map of LeConte Glacier camera set up (WorldView-2) from Keinholz et al. (2019)

3. Data and Methods

3.1 Data and Normalization

3.1.1 Time Lapse Imagery (Alaska)

Time-lapse imagery collected from Amundson et al. (2017) (DOI 10.18739/A2J38KJ1W) and used in Kienholz et al. (2019) had the initial intention of using optical flow for iceberg movement to derive current and flow patterns within LeConte Bay, Alaska. The bay was recorded in multiple sessions starting from April

2016 through September 2017. A follow up field campaign collected more images in September 2018 University of Alaska Southeast (2020) (DOI 10.18739/A27W6754N). Sampling intervals varied from 15 seconds up to 240 seconds. 5 cameras were set up along the bay to capture images from LeConte Glacier terminus to the mouth of the bay (several different locations). Figure 13 from Kienholz et al., 2019 shows the field of view for each of the cameras set up with the bay as well as included camera specs in Table 2. Collected images generally are taken during a 13-hour period from 14:00 to 3:00 (UTC). The only recurring dates between the years 2016-2018 is September 1-18th. Other recurring data only exists between 2016-2017 or 2017-2018. Some imagery files are neglected due to their longer sampling period (1 hour or 30 min).

Figure 14. Examples of LeConte camera views

Table 2. Summary of LeConte sampling information

Camera	Sample interval (s)	Year	# events observed
UAS1	120	2016, 2017	84, 49
UAS2	120	2016, 2017	72, 78
UAS3	120	2016, 2017	52, 44
UAS1hr	15	2017	20
UAS2hr	15	2017	12
UAS3hr	15	2017	16
UAS5_hr	15	2017	1
UAS5	60	2017	11
UAS6	15	2017	29
UAS7	30	2018	16
UAS8	30	2018	22
UAS9	30	2018	15
UAS10	30	2018	41

3.1.2 Time Lapse Imagery (Greenland)

Time-lapse imagery was used from our sites in Greenland along with existing data sets from LeConte Glacier campaigns from 2016-2018 provided by the Arctic Data Center (arcticdata.io). Greenland sites (QORQ, NIAQ, INKF) collected images at 1-to-3-minute intervals during hours with daylight. We use very low-cost 8 mega-pixel Arduino cameras at QORQ and INKF, while we use more expensive 8 mega-pixel video internet connected cameras with high quality lenses at NIAQ, UMNQ and UPI0. Images used for this study were taken from August through November 2025.

3.1.3 Iceberg Measurements

Unstable icebergs were sought out in time-lapse video and occurrence times were documented. From the sorted unstable events (Figure 15), the latest image prior to the event is separated and is used to collect the iceberg measurements. For a clearer example, if the image sampling interval is 30 seconds and an event is identified at 12:00:00, we would use the image taken at 11:59:30 to measure icebergs. Measurements derived from

the manual annotations include width and height. We use CVAT (Computer Vision Annotation Tool) an open-source annotating software, to measure and export iceberg measurements. The unit of iceberg measurements are in pixels. In Alaska, many more unstable events were found (compared to the Greenland sites) which may be attributed to the source glacier, higher sampling interval, observation points in proximity to the terminus, and the greater observation period.

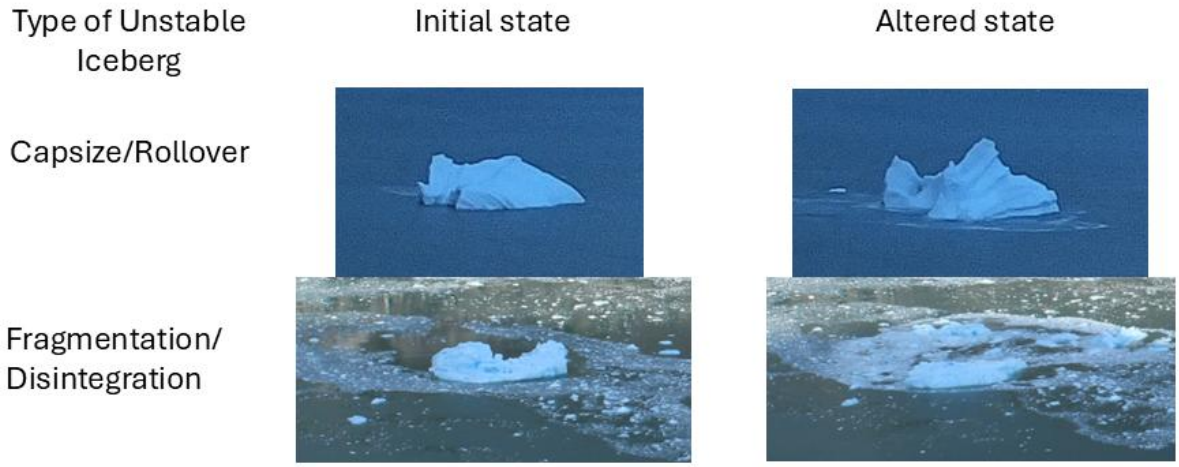

Figure 15. Images of initial and altered states of icebergs based on unstable event

3.1.4 Meteorological Data

To accompany the iceberg measurements, meteorological data was used from field data from (Amundson et al., 2017) (DOI 10.18739/A2J38KJ1W) and our site NIAQ. Hourly temperature readings are utilized in this study.

3.2 Workflow

The workflow for this study follows similar approaches for rare event studies. After data collection we clean and process the images. Cleaning consists of the removal of outliers, sampling (random split into training and test), and feature scaling (natural log transformation). From there the data is used in our chosen algorithmic approach: binary

logistic regression (LR). The model's performance is then evaluated using common performance metrics along with cross validation. Figure 16 shows the workflow for this study.

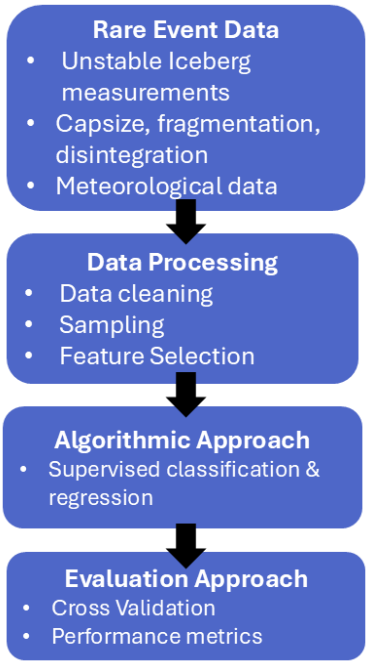

Figure 16. Flowchart showing workflow

3.3 Logistic Regression

Logistic regression (LR) is a well-known machine learning algorithm used for predicting the probability of an outcome. LR is comparable to linear regression in terms of finding relationships between dependent and independent variables. However, working with binary outcomes is more suited to using LR and uses the logistic equation. Another important characteristic of LR is that the data does not have to follow normal distribution.

$$p(x) = \frac{1}{1 + e^{-(\beta_0 + \beta_1 x)}}$$

We use scikit-learn's LR model in jupyter notebook to run our experiments. First, we apply our sampling method to achieve a more balanced dataset. We use RMU and

SMOTE to do this. The raw data is split into training (80%) and a test set (20%). Feature scaling using natural log is applied to each set and is used as input for the model. After the model is trained on the training set, we test the model and evaluate its performance. Model metrics include precision, accuracy, recall, F1 and Area Under the Curve (AUC).

3.4 Sampling

The compiled data sets for Alaska [0:2066, 1:479] and Greenland [0:104, 1:16] are imbalanced due to the rarity of unstable icebergs. We use sampling to mitigate the effects of the class imbalance to avoid the model overfitting. Sampling is applied after splitting the data into training and testing sets. We use two methods: Random Majority Undersampling (RMU) and Synthetic Minority Oversampling Technique (SMOTE) (Chawla et al., 2011). RMU randomly removes samples from the majority class to become more balanced compared to the minority class. Enough stable iceberg measurements were removed to match the quantity of unstable measurements for each study area. SMOTE creates synthetic minority points between existing minority neighboring points. Unstable measurements were generated to match the number of stable measurements for each respective site. A natural log transformation is applied after sampling.

4. Results and Interpretations

4.1 Iceberg Measurements (Alaska)

Icebergs were measured and annotated with labels describing their state of stability. The sample from LeConte glacier icebergs includes 2066 stable and 479 unstable labels. The rarity of unstable icebergs causes an imbalance in the dataset. We use Random Majority Undersampling (RMU) to address these issues despite the

drawback of potentially underfitting the model and a more advanced technique Synthetic Minority Oversampling Technique (SMOTE) (Chawla et al., 2011). The initial Alaska raw data of width and height measurements follow a log normal distribution. Both histograms shown in Figure 17 are heavily skewed and have long right tails which are not characteristics of a normal distribution. Feature scaling was applied to the raw measurements by using natural log transformations. These scaled values are used for the remainder of the study. Figure 17 also shows the normal distribution of ln(width) and ln(height) and fits in apparent outliers. In the ln(width) plot the stable icebergs have a mean of ~4.14 but the unstable icebergs are shifted slightly to the right with a mean of ~4.68. A similar pattern can be seen in the ln(height) plot as well with stable mean of 3.11 and unstable mean of 3.69. Table 3 has descriptive statistics for each curve.

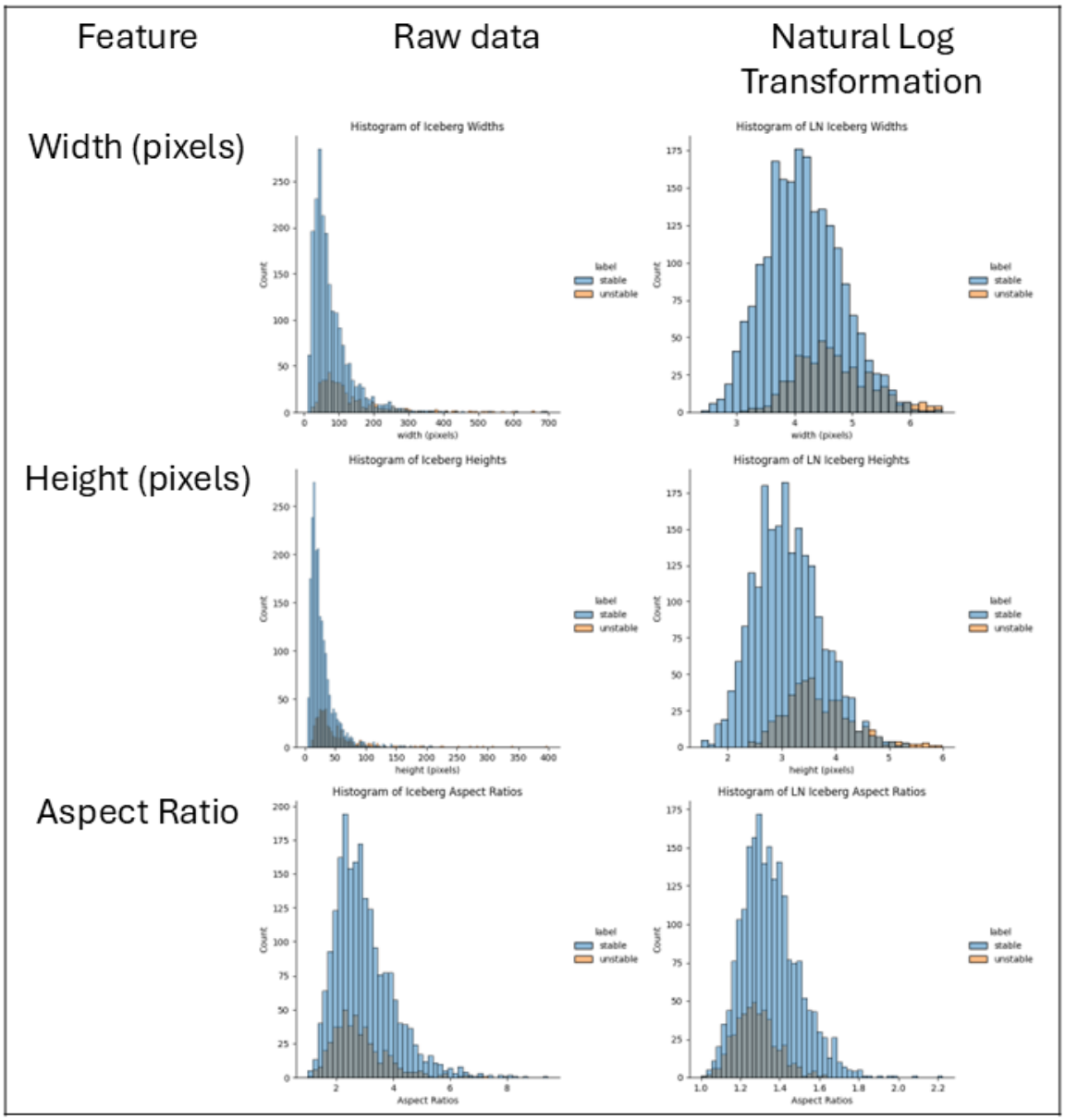

Figure 17. Histograms of LeConte iceberg measurements (width, height and aspect ratio) in pixels. Raw data (left) versus natural log transformation (right)

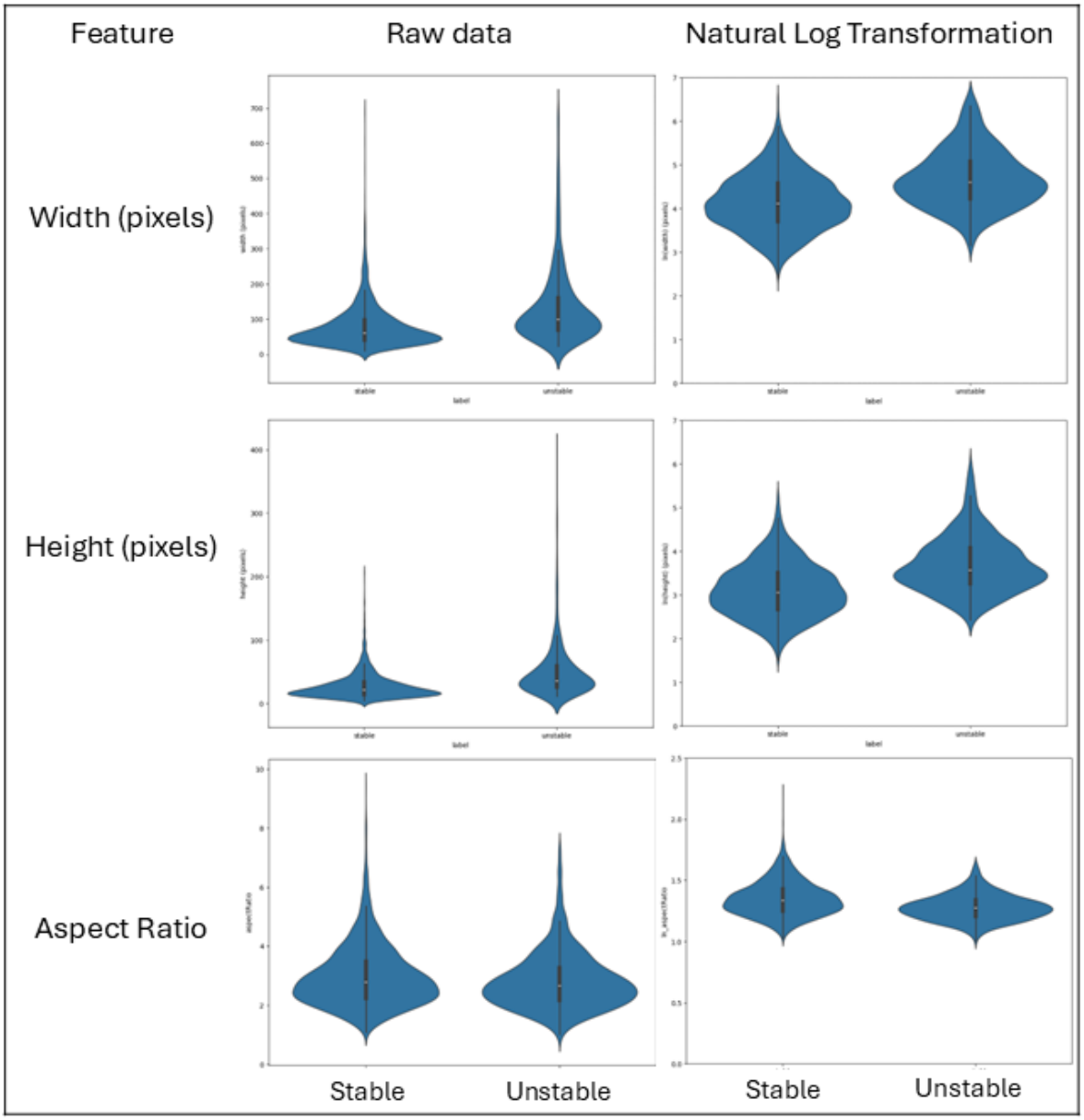

Figure 18. Violin plots for Alaska iceberg measurements. Raw data (left) versus natural log transformation (right)

Table 3. Descriptive statistics for Alaska

	ln(height) stable	ln(height) unstable	ln(width) stable	ln(width) unstable
count	2066	479	2066	479
mean	3.112201	3.692765	4.147551	4.679146
std	0.617947	0.633679	0.647609	0.655445
min	1.504077	2.431857	2.394252	3.161247
25%	2.672941	2.431857	3.705245	4.225738
50%	3.055651	3.562182	4.110792	4.600861
75%	3.512441	4.072095	4.581210	5.075387
max	5.336335	5.987833	6.547675	6.535532

To further explore this distinction, we use violin plots and scatterplots. Violin plots show the population density of the different classes and measurements (Figure 18). Stable icebergs have a denser population and higher occurrence with lower height and width measurements. Unstable icebergs, by contrast have a more elongated population and, generally, greater height and width measurements. There is an area of overlap which could cause confusion within predictions. Even decreasing the population of the stable icebergs, the slight shift of the population curve to the right in the unstable icebergs is apparent. However, when inspecting the aspect ratios of both, they are extremely similar and do not seem to have any indication that can be used for distinction.

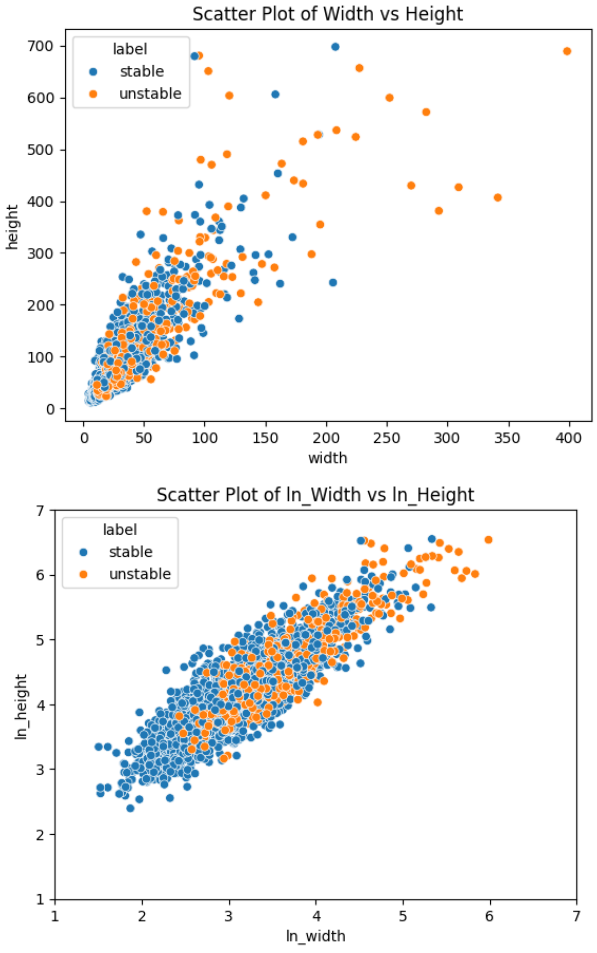

Figure 19. Scatterplots for Alaska icebergs

Figure 19 shows a scatterplot of ln(width) vs. ln(height) to visualize how the spatial distribution of iceberg sizes. In the plot we see an intersect of stable and unstable points but with stable points extending further to zero and unstable points continuing away from 0.

4.2 Iceberg Measurements (Greenland)

For Greenland icebergs data is much sparser compared to Alaska due to the shorter temporal coverage (~ 3 months) so we compile iceberg measurements from sites UMNQ, NIAQ and QORQ. Despite getting iceberg measurements from various locations, we observe similar patterns to LeConte. Both histograms shown in Figure 20 are heavily skewed and have long right tails which are not characteristics of a normal distribution. Feature scaling was applied to the raw measurements by using natural log transformations. These scaled values are used for the remainder of the study. The normal distribution of ln(width) and ln(height) fits in apparent outliers. In the ln(width) plot the stable icebergs have a mean of ~4.62 but the unstable icebergs are shifted almost a whole point more to the right with a mean of ~5.48. Again, a similar pattern can be seen in the ln(height) plot as well with stable mean of ~3.74 and unstable mean of ~4.48. Table 4 has descriptive statistics for each curve.

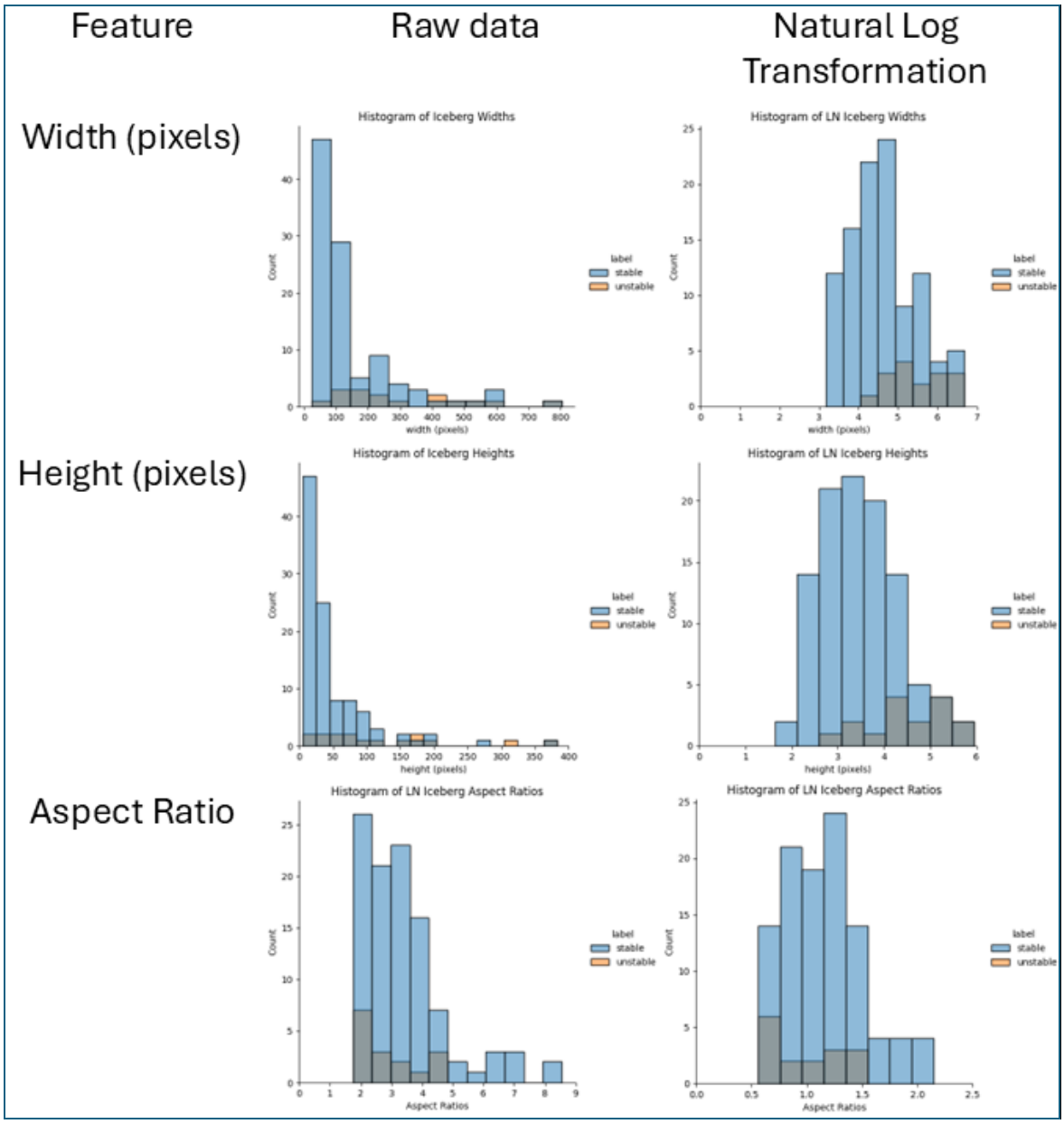

Figure 20. Histograms for Greenland iceberg measurements (width, length and aspect ratio). Raw data (left) versus natural log transformation (right)

To further explore this distinction, we use violin plots and scatterplots. Violin plots show the population density of the different classes and measurements (Figure 21). Stable icebergs have a denser population and higher occurrence with lower height and

width measurements. Unstable icebergs, by contrast have a more elongated population and, generally, greater height and width measurements.

Table 4. Descriptive statistics for Greenland

	ln(height) stable	ln(height) Unstable	ln(width) stable	ln(width) unstable
count	104	104	16	16
mean	3.470873	4.480303	4.620902	5.482230
std	0.857569	0.880893	0.811847	0.703301
min	1.637053	3.021887	3.170526	4.409885
25%	2.891850	3.989035	4.010058	4.409885
50%	3.304046	4.447471	4.521888	5.385960
75%	4.019172	5.147084	5.232139	6.016836
max	5.949261	5.907458	6.689226	6.672008

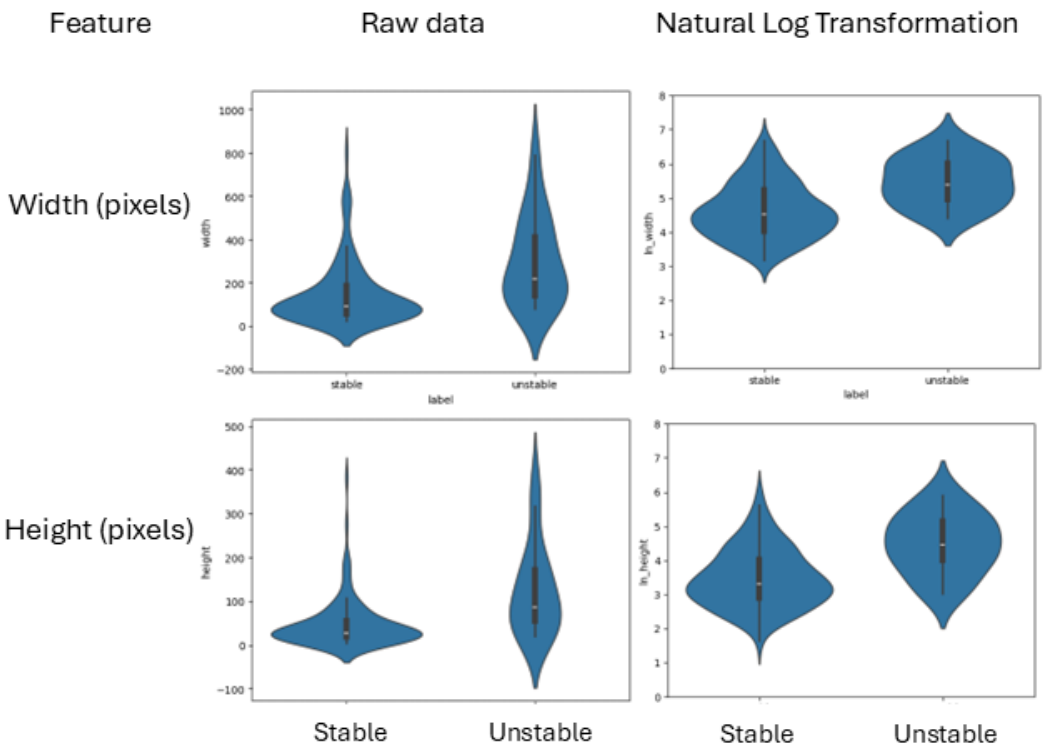

Figure 21. Violin plots of Greenland iceberg measurements (width and length). Raw data (left) versus natural log transformation (right)

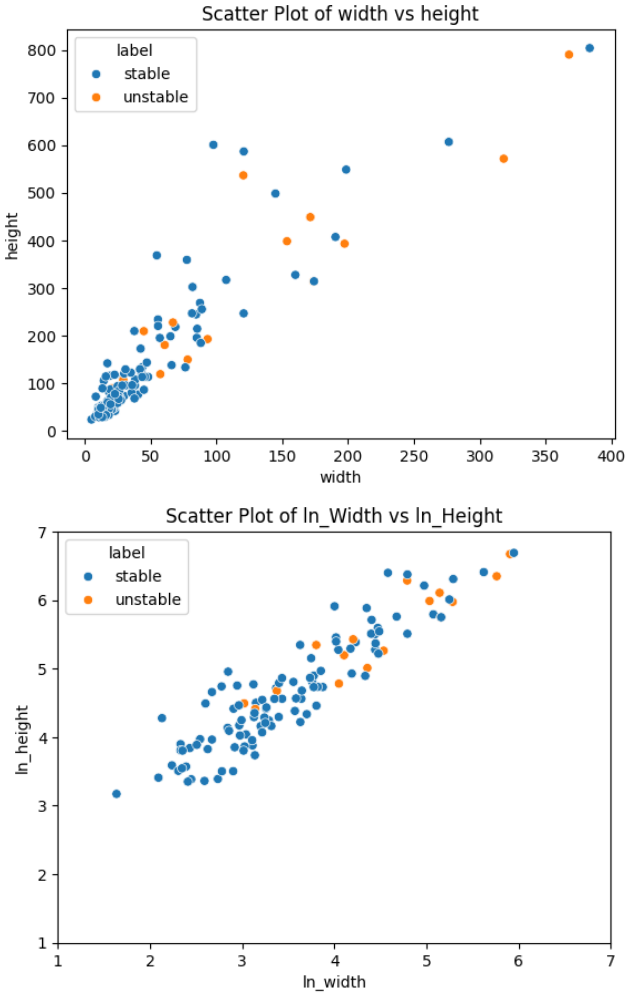

Figure 22. Scatterplots for Greenland icebergs

4.3 Logistic Regression (Alaska)

In this section we evaluate the LR model's performance for each sampling technique (Table 5). Before training the model, we use sampling techniques RMU to randomly remove data belonging to the majority class (stable) and SMOTE to create synthetic data for the minority class (unstable). These methods attempt to mitigate the imbalance between the classes. LR may show implications that iceberg measurements can be used to differentiate iceberg stability. All the models performed better comparatively to having no skill. The applied sampling techniques slightly improved the

AUC score compared to no sampling. The predicted probabilities show the model implies that larger measurements are more likely to be unstable than small measurements.

Table 5. Alaska logistic regression model metrics based on sampling method

	None	RMU	SMOTE
Model Score	85.07%	65.10%	66.14%
AUC Score	0.718	0.739	0.736
Confusion Matrix	[[426 11] [65 7]]	[[56 30] [37 69]]	[[306 130] [150 241]]
Precision			
0	0.87	0.59	0.67
1	0.39	0.70	0.65
Recall			
0	0.97	0.67	0.70
1	0.10	0.62	0.62
F1			
0	0.92	0.63	0.69
1	0.16	0.66	0.63
5-fold cross-validation scores	[0.81, 0.82, 0.82, 0.81, 0.78]	[0.72, 0.70, 0.67, 0.73, 0.62]	[0.66, 0.67, 0.66, 0.65, 0.68]

4.4 Logistic Regression (Greenland)

In this section we evaluate the LR model's performance for each sampling technique (Table 6). Before training the model, we use sampling techniques RMU to randomly remove data belonging to the majority class (stable) and SMOTE to create synthetic data for the minority class (unstable). The model metrics for Greenland skeptically show the models with near perfect scores. However, closer observation of the model's prediction values and classification reveals the models classify the test sets as almost entirely stable. This may be attributed to the extremely small size of the dataset for Greenland. If the Greenland dataset were more similar in size to Alaska, we predict the models would behave similarly to the Alaska models. LR is seemingly unable to give any deeper insights into this data.

Table 6. Greenland logistic regression model metrics based on sampling method

	None	RMU	SMOTE
Model Score	79.16%	57.14%	80.10%
AUC Score	0.937	1.00	0.884
Confusion Matrix	[[19 0] [5 0]]	[[3 0] [3 1]]	[[16 5] [3 18]]
Precision			
0	0.79	0.50	0.67
1	0.00	1.00	0.65
Recall			
0	1.00	1.00	0.70
1	0.00	0.25	0.62
F1			
0	0.88	0.67	0.69
1	0.00	0.40	0.63
5-fold cross-validation scores	[0.88, 0.92, 0.88, 0.70, 0.83]	[0.6, 0.8, 0.6, 0.8, 0.8]	[0.66, 0.67, 0.66, 0.65, 0.68]

4.5 Time Series (Alaska)

We observe the occurrence of events through time series for each station and compare against air temperature if available.

2016 air temperature (Figure 23) observations see a general increase from April to mid-July with a maximum temperature of 20 °C. The remainder of July, August, and the beginning of September the air temperature remains relatively steady approximately between 10 °C and 15 °C. We see temperatures begin and continue to fall from September to October. Looking at the 2016 occurrences (Figure 24), we see days with the most events occurring in April, August and September. From May through July, it appears there are fewer events and not many multiples are occurring.

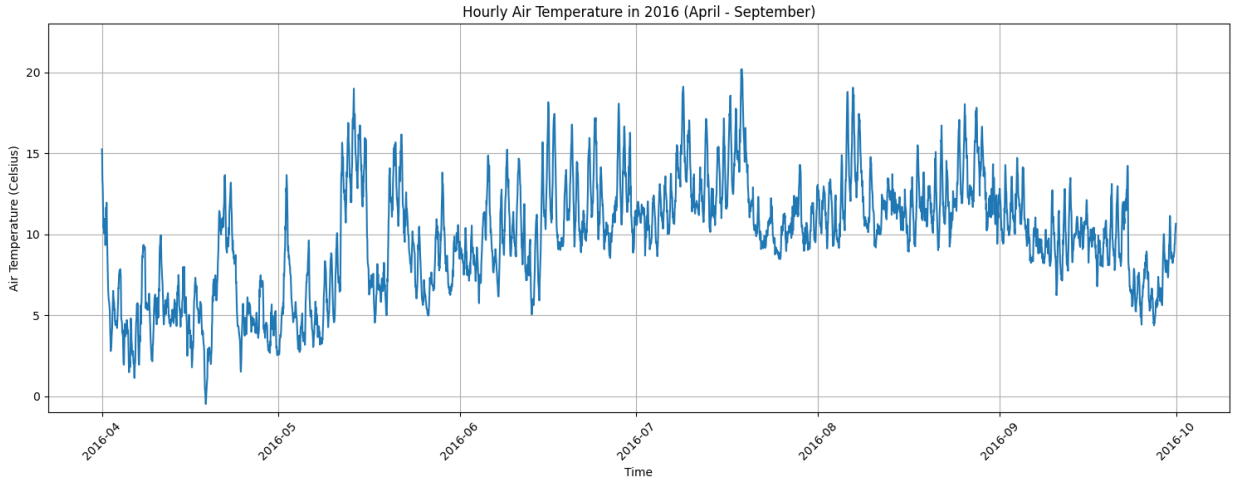

Figure 23. Time series plot for LeConte hourly air temperature in 2016 (April - September)

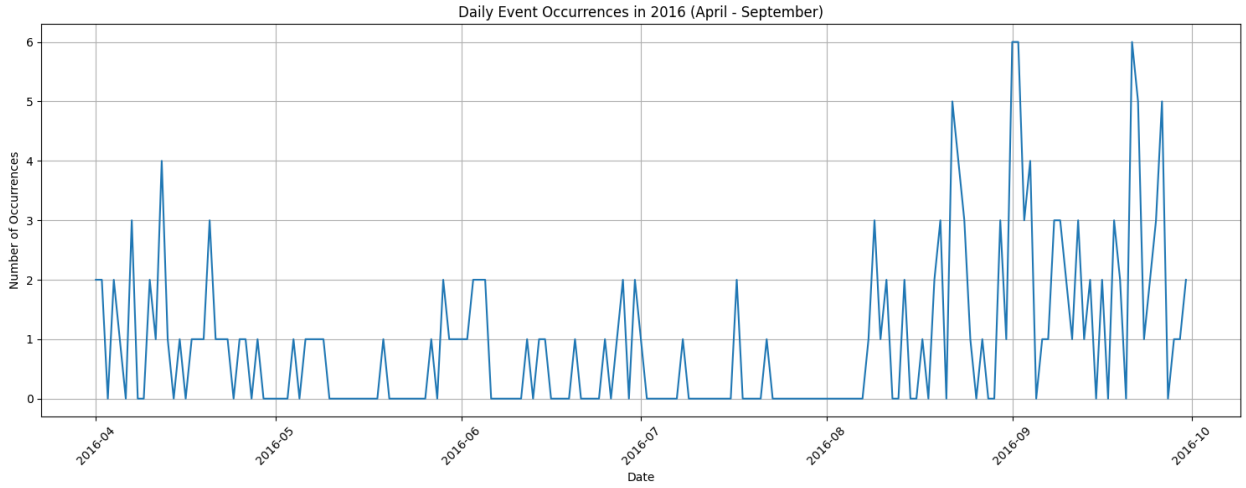

Figure 24. Time series plot for daily event occurrence in 2016 (April - September)

2017 air temperature observations (Figure 25) see an increase from mid-June to August with a maximum temperature slightly above 20 °C. In mid-August and beginning of September we observe spikes in temperature. Events in 2017 (Figure 28) do not appear to have any trend.

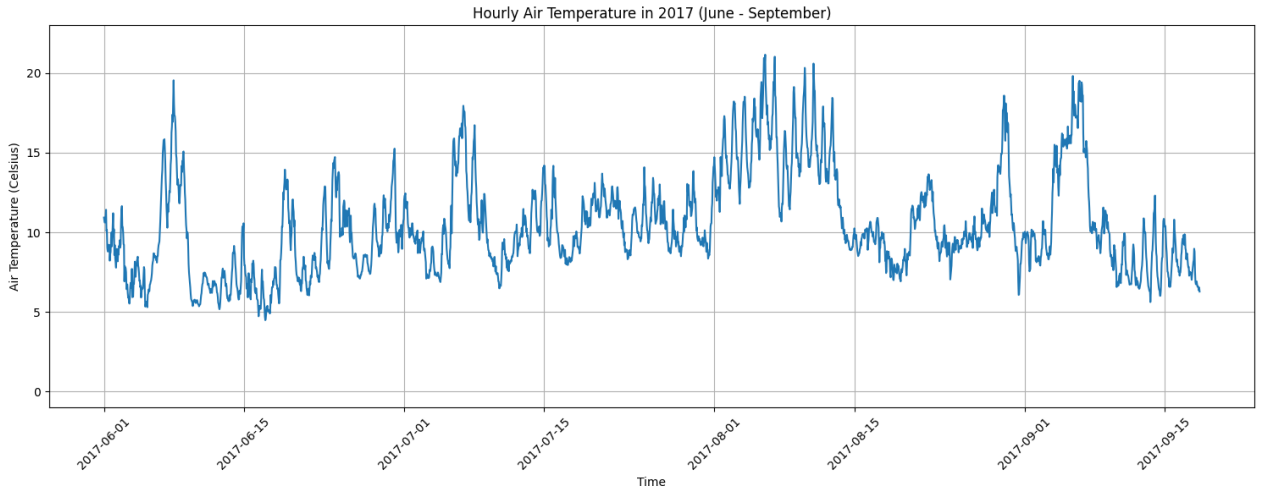

Figure 25. Time series plot for LeConte hourly air temperature in 2017 (June - September)

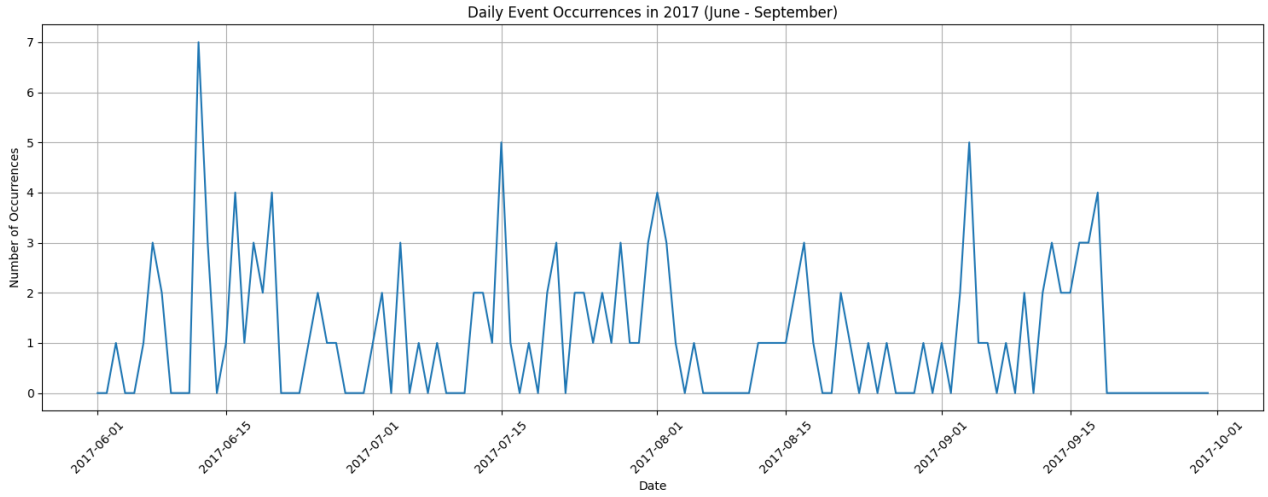

Figure 26. Time series plot for daily event occurrence in 2017 (June - September)

2018 event time series (Figure 27) is a shorter temporal range, however compared to 2016 and 2017 events there are generally more events. Again, there is seemingly no observable pattern.

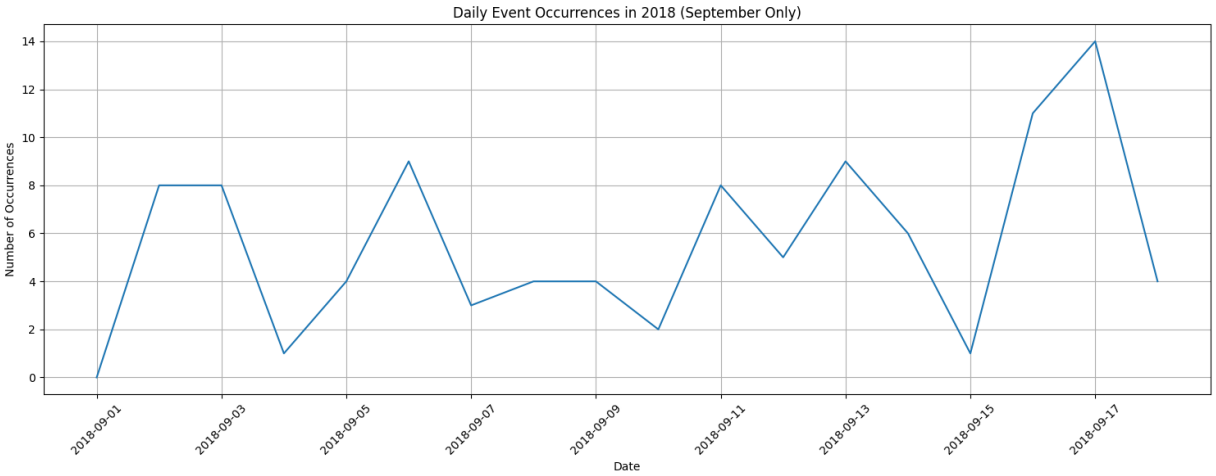

Figure 27. Time series plot for daily event occurrence in 2018 (September Only)

4.6 Time Series (Greenland)

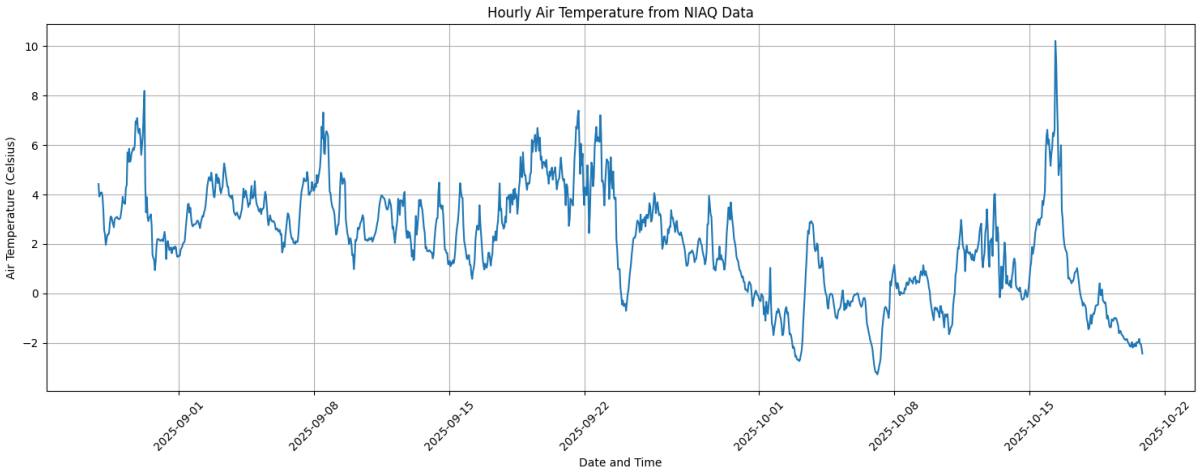

Figure 28. Time series plot of NIAQ hourly air temperature (September - October)

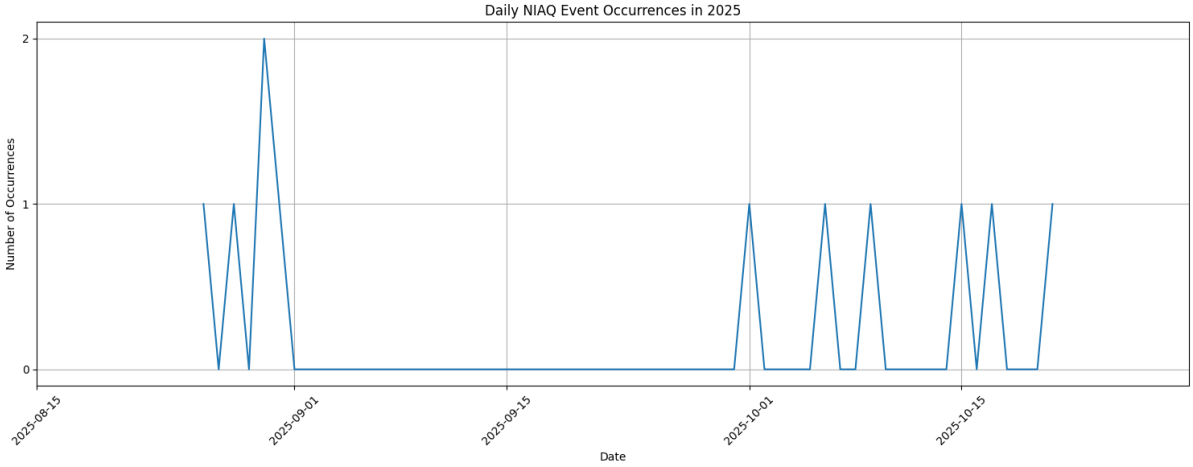

Figure 29. Time series plot for NIAQ daily event occurrences

Temperature measurements at NIAQ in September remain between about 2-6 °C. October sees lower temperatures and occasionally dropping to -2 °C. From the event time series, most occur in October with a couple occurring at the end of August.

UMNQ and QORQ have different temporal ranges and have no weather stations. UMNQ has most events occurring in the beginning of November. QORQ only had events in August.

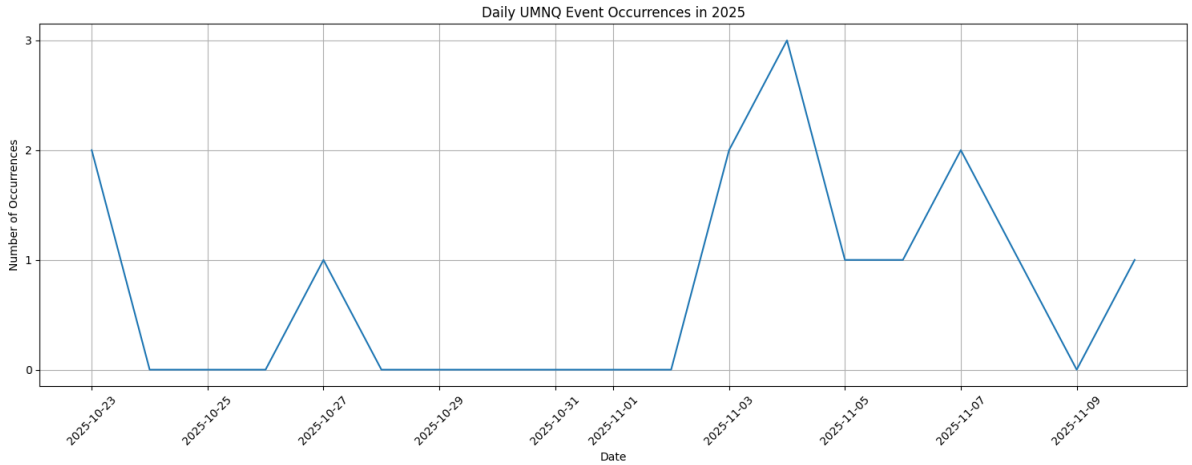

Figure 30. Time series plot for UMNQ daily event occurrences

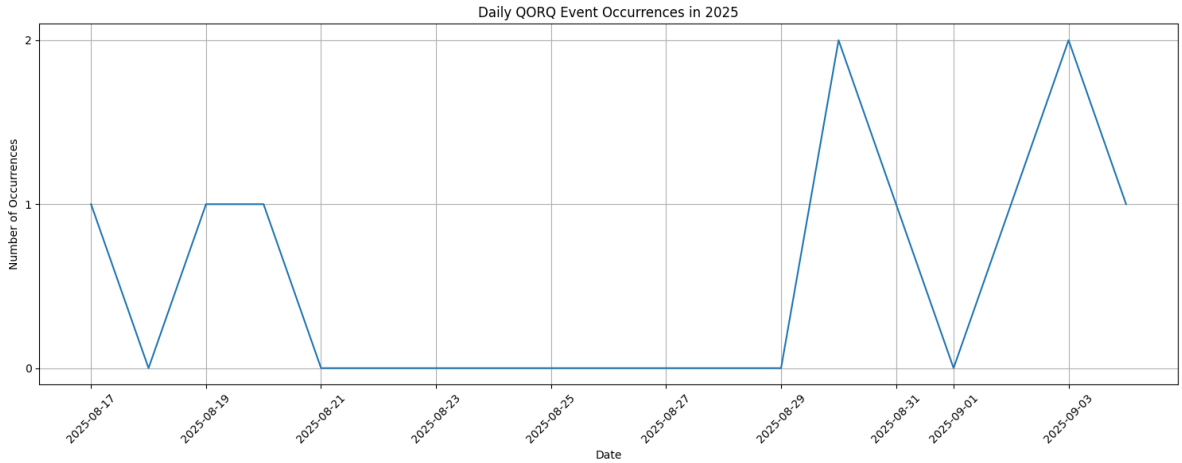

Figure 31. Time series plot for QORQ daily event occurrences

5. Discussion

This study is focused on attempting to predict an iceberg's stability based on its measurements relative to other icebergs within the population. We initially thought the aspect ratio of the measurement would be the determining factor on iceberg stability but found using the width and height measurements as separate inputs for training resulted in improved predictions. Pertaining to the air temperature time-series, a more likely useful measurement would be water temperatures. However, these measurements are difficult to obtain.

For both iceberg populations at Alaska and Greenland we observe a log normal distribution, which agrees with other iceberg studies like Enderlin et al. (2016), Sulak et al. (2017) and Scheick et al. (2023). Despite these studies using top-down satellite imagery, it would make sense that proportions of an iceberg would remain similar from a different perspective. What we also find interesting is the similarity between the distribution of the stable and unstable icebergs from both sites. Both show the unstable icebergs tend to have relatively larger measurements compared to the stable ones. We did not perform any statistical tests to confirm this finding is significant but is interesting for prospects.

While the general iceberg measurements make sense, it becomes more difficult to compare our results due to the lack of similar studies. Like Burton et al.'s (2012) we study iceberg stability and iceberg measurements. However, they identify a clear-cut boundary between stable and unstable synthetic rectangular icebergs. In contrast, we measure real icebergs and find there is much overlap between stable and unstable icebergs. This difference could also be attributed to our study not knowing the true

height of the iceberg. Enderlin et al. (2016) used digital elevation models of icebergs to estimate the submerged portion of icebergs (draft) assuming hydrostatic equilibrium.

In Ke et al.'s (2023) exponential smoothing was used to predict iceberg tsunami events with tide amplitude and event occurrences. Since we did not have any amplitude data to work with, we attempted to use air temperature and event occurrences. However, we suspect that water temperature, bathymetry, wind and waves may have more influence on iceberg stability. Abib et al. (2023) states the similar water temperature conditions for LeConte are comparable to Greenland during the melt season.

When comparing when the events are happening, between the different sites, Alaska has significantly more. We believe the most significant difference between the sites is the proximity to the glacier front. At LeConte, the cameras sites are proximal and are more likely to experience the direct effects of glacier calving. Compared to our Greenland sites, where they are distal from the terminus face but closer to towns. There may be different external dynamics that influence iceberg stability mechanisms that we did not consider, that could be of interest. The complexity of iceberg shapes was neglected as well and could also be a reason for different chances of being unstable. Simulating melting icebergs that have travelled from the glacier front is also something that might be useful. How far an iceberg travels from the glacier front might also have some implications on an icebergs' lifespan and stability. Coupling hydrodynamic models like in Bonnet et al (2020) and Heller et al. (2021) with real iceberg measurements would also be of interest and could simulate predicted iceberg drafts.

The logistic regression models within this study would not be applicable to real-life scenarios. In both cases of Alaska and Greenland, the models improved when applying sampling techniques. However, the set proportions used to train, and test are no representative compared to actual sites. We suspect that a possible hybrid of under and over sampling could better balance the set.

6. Conclusion

This study is a starting point for investigating a potential method to monitor iceberg capsize. Sites in Greenland and Alaska collect samples of iceberg sizes (widths and heights) from ground imagery. We investigated the relationships of iceberg stability with iceberg sizes and weather data. This study concludes there may be a relationship between the visible portion of an iceberg and its stability, with generally larger icebergs more likely to be unstable. We also find that it is not likely that there are implications for air temperature having influence on iceberg stability.

This study is designed to be a stepping-stone towards the eventual development of an autonomous model to evaluate the chances of iceberg capsize and local tsunami genesis. Before expending effort towards a system, we need to confirm a signal exists between unstable icebergs and their measurements. More data should be collected, especially for the Greenland sites to create a robust iceberg monitoring system. Implementing additional variables should also be considered (water surface temperature, bathymetry, etc.). The exploration of non-linear regression which would allow for more flexibility on finding the best-fitting curve. Future work includes using a coupled system between a regression model and live camera feed to calculate the probability of an iceberg flipping in real time.

Complexities should be implemented in future studies including iceberg morphology. This study simplified the iceberg shapes into rectangles, as compared to keeping their complex shapes. Semantic segmentation could be implemented in future studies to classify more complex iceberg shapes and extract detailed features. More complexity is to consider are icebergs that capsize multiple times and iceberg movement (spinning or sinking slowly).

We also recognize there are uncertainties within the study. There is a lack of capsizing iceberg data and future studies may consider using augmentation methods on existing data. Another important uncertainty is within the measurements of the icebergs. With the lack of camera parameters from all sets of images, we were unable to get relatable units of measurements. The measurement calculations were based on how many pixels the iceberg occupies in the picture. All our sites in Greenland have stereo cameras, and when calibrated correctly these should provide accurate iceberg measurements.

References

Abib, N., Sutherland, D. A., Amundson, J. M., Duncan, D., Eidam, E. F., Jackson, R. H., Kienholz, C., Morlighem, M., Motyka, R. J., Nash, J. D., Ovall, B., & Pettit, E. C. (2023). Persistent overcut regions dominate the terminus morphology of a rapidly melting tidewater glacier. *Annals of Glaciology*, 64(90), 1–12. https://doi.org/10.1017/aog.2023.38

Amundson, J., Kienholz, C., Motyka, R., Sutherland, D., Nash, J., & Jackson, R. (2017a). *LeConte Glacier meteorological data 2016-2017, Alaska* [Text/xml]. NSF Arctic Data Center. https://doi.org/10.18739/A2NV99B85

Amundson, J., Kienholz, C., Motyka, R., Sutherland, D., Nash, J., & Jackson, R. (2017b). *LeConte Glacier time-lapse photos 2016-2017, Alaska* [Text/xml]. NSF Arctic Data Center. https://doi.org/10.18739/A2J38KJ1W

Aschwanden, A., Fahnestock, M. A., Truffer, M., Brinkerhoff, D. J., Hock, R., Khroulev, C., Mottram, R., & Khan, S. A. (2019). Contribution of the Greenland Ice Sheet to sea level over the next millennium. *Science Advances*, *5*(6), eaav9396. https://doi.org/10.1126/sciadv.aav9396

Berg, D., Barletta, V. R., Hassan, J., Lippert, E. Y. H., Colgan, W., Bevis, M., Steffen, R., & Khan, S. A. (2024). Vertical Land Motion Due To Present-Day Ice Loss From Greenland's and Canada's Peripheral Glaciers. *Geophysical Research Letters*, *51*(2), e2023GL104851. https://doi.org/10.1029/2023GL104851

Bolch, T., Sandberg Sørensen, L., Simonsen, S. B., Mölg, N., Machguth, H., Rastner, P., & Paul, F. (2013). Mass loss of Greenland's glaciers and ice caps 2003–2008 revealed from ICESat laser altimetry data. *Geophysical Research Letters*, *40*(5), 875–881. https://doi.org/10.1002/grl.50270

Bollen, K. E., Enderlin, E. M., & Muhlheim, R. (2023). Dynamic mass loss from Greenland's marine-terminating peripheral glaciers (1985–2018). *Journal of Glaciology*, *69*(273), 153–163. https://doi.org/10.1017/jog.2022.52

Bonnet, P., Yastrebov, V. A., Queutey, P., Leroyer, A., Mangeney, A., Castelnau, O., Sergeant, A., Stutzmann, E., & Montagner, J.-P. (2020). Modelling capsizing icebergs in the open ocean. *Geophysical Journal International*, *223*(2), 1265–1287. https://doi.org/10.1093/gji/ggaa353

Burton, J. C., Amundson, J. M., Abbot, D. S., Boghosian, A., Cathles, L. M., Correa-Legisos, S., Darnell, K. N., Guttenberg, N., Holland, D. M., & MacAyeal, D. R. (2012). Laboratory investigations of iceberg capsize dynamics, energy dissipation and tsunamigenesis. *Journal of Geophysical Research: Earth Surface*, *117*(F1), 2011JF002055. https://doi.org/10.1029/2011JF002055

Chawla, N. V., Bowyer, K. W., Hall, L. O., & Kegelmeyer, W. P. (2011). *SMOTE: Synthetic Minority Over-sampling Technique*. https://doi.org/10.48550/ARXIV.1106.1813

Chudley, T. R., Howat, I. M., King, M. D., & MacKie, E. J. (2025). Increased crevassing across accelerating Greenland Ice Sheet margins. *Nature Geoscience*. https://doi.org/10.1038/s41561-024-01636-6

Cubbin, C. (2025, July 11). Greenland village wakes up to titanic iceberg dangerously close to homes. *New York Post*. https://nypost.com/2025/07/11/science/massive-iceberg-headed-toward-greenland-sparks-official-warning/

De La Garza, A. (2018, July 16). A Massive Iceberg Is Threatening to Destroy a Village in Greenland. *Time*. https://time.com/5339726/massive-iceberg-village-greenland/

Ding, S., Zeng, D., Zhou, L., Han, S., Li, F., & Wang, Q. (2023). Multi-Scale Polar Object Detection Based on Computer Vision. *Water*, *15*(19), 3431. https://doi.org/10.3390/w15193431

Enderlin, E. M., Hamilton, G. S., Straneo, F., & Sutherland, D. A. (2016). Iceberg meltwater fluxes dominate the freshwater budget in Greenland's iceberg-congested glacial fjords. *Geophysical Research Letters*, *43*(21). https://doi.org/10.1002/2016GL070718

European Space Agency. (2018, July 17). *Looming iceberg* [International]. The European Space Agency. https://www.esa.int/ESA_Multimedia/Images/2018/07/Looming_iceberg

Fahrner, D., Lea, J. M., Brough, S., Mair, D. W. F., & Abermann, J. (2021). Linear response of the Greenland ice sheet's tidewater glacier terminus positions to climate. *Journal of Glaciology*, *67*(262), 193–203. https://doi.org/10.1017/jog.2021.13

FitzMaurice, A., Cenedese, C., & Straneo, F. (2017). Nonlinear response of iceberg side melting to ocean currents. *Geophysical Research Letters*, *44*(11), 5637–5644. https://doi.org/10.1002/2017GL073585

Fritz, M., Vonk, J. E., & Lantuit, H. (2017). Collapsing Arctic coastlines. *Nature Climate Change*, *7*(1), 6–7. https://doi.org/10.1038/nclimate3188

Greene, C. A., Gardner, A. S., Wood, M., & Cuzzone, J. K. (2024). Ubiquitous acceleration in Greenland Ice Sheet calving from 1985 to 2022. *Nature*, *625*(7995), 523–528. https://doi.org/10.1038/s41586-023-06863-2

Hansen, K., & Carlowicz, M. (2018). *Iceberg Towers over Innaarsuit* [Government]. NASA Earth Observatory. https://earthobservatory.nasa.gov/images/92443/iceberg-towers-over-innaarsuit

Heller, V., Attili, T., Chen, F., Gabl, R., & Wolters, G. (2021). Large-scale investigation into iceberg-tsunamis generated by various iceberg calving mechanisms. *Coastal Engineering*, *163*, 103745. https://doi.org/10.1016/j.coastaleng.2020.103745

Heller, V., Chen, F., Brühl, M., Gabl, R., Chen, X., Wolters, G., & Fuchs, H. (2019). Large-scale experiments into the tsunamigenic potential of different iceberg calving mechanisms. *Scientific Reports*, *9*(1), 861. https://doi.org/10.1038/s41598-018-36634-3

Hester, E. W., McConnochie, C. D., Cenedese, C., Couston, L.-A., & Vasil, G. (2021). Aspect ratio affects iceberg melting. *Physical Review Fluids*, *6*(2), 023802. https://doi.org/10.1103/PhysRevFluids.6.023802

Hofer, S., Lang, C., Amory, C., Kittel, C., Delhasse, A., Tedstone, A., & Fettweis, X. (2020). Greater Greenland Ice Sheet contribution to global sea level rise in CMIP6. *Nature Communications*, *11*(1), 6289. https://doi.org/10.1038/s41467-020-20011-8

Kc, A., Enderlin, E. M., Fahrner, D., Moon, T., & Carroll, D. (2025). Seasonality in terminus ablation rates for the glaciers in Greenland (Kalaallit Nunaat). *The Cryosphere*, *19*(8), 3089–3106. https://doi.org/10.5194/tc-19-3089-2025

Ke, H., Ai, S., Yan, B., Zhou, C., Wang, Z., Yang, Y., Liu, T., An, J., & Chen, Y. (2022). Iceberg-Induced Tsunamis Near Dålk Glacier, Antarctica. *Journal of Surveying Engineering*, *148*(1), 04021027. https://doi.org/10.1061/(ASCE)SU.1943-5428.0000385

Kienholz, C., Amundson, J. M., Motyka, R. J., Jackson, R. H., Mickett, J. B., Sutherland, D. A., Nash, J. D., Winters, D. S., Dryer, W. P., & Truffer, M. (2019). Tracking icebergs with time-lapse photography and sparse optical flow, LeConte Bay, Alaska, 2016–2017. *Journal of Glaciology*, *65*(250), 195–211. https://doi.org/10.1017/jog.2018.105

Kim, E., Dahiya, G. S., Løset, S., & Skjetne, R. (2019). Can a computer see what an ice expert sees? Multilabel ice objects classification with convolutional neural networks. *Results in Engineering*, *4*, 100036. https://doi.org/10.1016/j.rineng.2019.100036

Koo, Y., Xie, H., Mahmoud, H., Iqrah, J. M., & Ackley, S. F. (2023). Automated detection and tracking of medium-large icebergs from Sentinel-1 imagery using Google Earth Engine. *Remote Sensing of Environment*, *296*, 113731. https://doi.org/10.1016/j.rse.2023.113731

Lewis, S. (2025, July 11). Greenland coastal village bracing for potential collision with giant iceberg. *National Post*. https://nationalpost.com/news/world/greenland-coastal-village-bracing-for-potential-collision-with-giant-iceberg

Long, A. J., Szczuciński, W., & Lawrence, T. (2015). Sedimentary evidence for a mid-Holocene iceberg-generated tsunami in a coastal lake, west Greenland. *Arktos*, *1*(1), 6. https://doi.org/10.1007/s41063-015-0007-7

MacAyeal, D. R., Abbot, D. S., & Sergienko, O. V. (2011). Iceberg-capsize tsunamigenesis. *Annals of Glaciology*, *52*(58), 51–56. https://doi.org/10.3189/172756411797252103

MacFarlane, D. (2018, July 15). *11-Million-Ton Iceberg Stalls Offshore, Threatening Greenland Village*. The Weather Channel. https://weather.com/news/news/2018-07-15-greenland-massive-iceberg-innaarsuit

McCann, C. (2021, January 14). *Residents Displaced by a Mega-Tsunami Can Never Go Home*. Vice. https://www.vice.com/en/article/residents-displaced-by-a-mega-tsunami-can-never-go-home/

Minor, K., Agneman, G., Davidsen, N., Kleemann, N., Markussen, U., Lassen, D. D., & Rosing, M. T. (2019). *Greenlandic Perspectives on Climate Change 2018–2019: Results from a National Survey*. University of Greenland and University of Copenhagen. https://ssrn.com/abstract=3667214

Minor, K., Jensen, M. L., Hamilton, L., Bendixen, M., Lassen, D. D., & Rosing, M. T. (2023). Experience exceeds awareness of anthropogenic climate change in Greenland. *Nature Climate Change*, *13*(7), 661–670. https://doi.org/10.1038/s41558-023-01701-9

Møller, J. (2012, July 21). Iceberg "tsunami" off Greenland. *BBC News*. https://www.bbc.com/news/av/science-environment-18940497

Morlighem, M., Williams, C. N., Rignot, E., An, L., Arndt, J. E., Bamber, J. L., Catania, G., Chauché, N., Dowdeswell, J. A., Dorschel, B., Fenty, I., Hogan, K., Howat, I., Hubbard, A., Jakobsson, M., Jordan, T. M., Kjeldsen, K. K., Millan, R., Mayer, L., … Zinglersen, K. B. (2017). BedMachine v3: Complete Bed Topography and Ocean Bathymetry Mapping of Greenland From Multibeam Echo Sounding Combined With Mass Conservation. *Geophysical Research Letters*, *44*(21). https://doi.org/10.1002/2017GL074954

Nias, I. J., Nowicki, S., Felikson, D., & Loomis, B. (2023). Modeling the Greenland Ice Sheet's Committed Contribution to Sea Level During the 21st Century. *Journal of Geophysical Research: Earth Surface*, *128*(2), e2022JF006914. https://doi.org/10.1029/2022JF006914

Normandeau, A., MacKillop, K., Macquarrie, M., Richards, C., Bourgault, D., Campbell, D. C., Maselli, V., Philibert, G., & Clarke, J. H. (2021). Submarine landslides triggered by iceberg collision with the seafloor. *Nature Geoscience*, *14*(8), 599–605. https://doi.org/10.1038/s41561-021-00767-4

Osco, L. P., Wu, Q., De Lemos, E. L., Gonçalves, W. N., Ramos, A. P. M., Li, J., & Marcato, J. (2023). The Segment Anything Model (SAM) for remote sensing applications: From zero to one shot. *International Journal of Applied Earth Observation and Geoinformation*, *124*, 103540. https://doi.org/10.1016/j.jag.2023.103540

Paddison, L. (2024, September 13). *A landslide triggered a 650-foot mega-tsunami in Greenland. Then came something inexplicable*. CNN. https://www.cnn.com/2024/09/13/climate/mega-tsunami-landslide-greenland-seismic-signal

Poinar, K., Mankoff, K. D., Fausto, R. S., Fettweis, X., Loomis, B. D., Wehrlé, A., Jensen, C. D., Tedesco, M., Box, J. E., & Mote, T. L. (2023). *NOAA Arctic Report Card 2023: Greenland Ice Sheet*. https://doi.org/10.25923/YETX-RS76

Scheick, J., Enderlin, E. M., & Hamilton, G. (2019). Semi-automated open water iceberg detection from Landsat applied to Disko Bay, West Greenland. *Journal of Glaciology*, *65*(251), 468–480. https://doi.org/10.1017/jog.2019.23

Shankar, S., Stearns, L. A., & Van Der Veen, C. J. (2024). Semantic segmentation of glaciological features across multiple remote sensing platforms with the Segment Anything Model (SAM). *Journal of Glaciology*, *70*, e4. https://doi.org/10.1017/jog.2023.95

Shepherd, A., Ivins, E. R., A, G., Barletta, V. R., Bentley, M. J., Bettadpur, S., Briggs, K. H., Bromwich, D. H., Forsberg, R., Galin, N., Horwath, M., Jacobs, S., Joughin, I., King, M. A., Lenaerts, J. T. M., Li, J., Ligtenberg, S. R. M., Luckman, A., Luthcke, S. B., … Zwally, H. J. (2012). A Reconciled Estimate of Ice-Sheet Mass Balance. *Science*, *338*(6111), 1183–1189. https://doi.org/10.1126/science.1228102

Sherriff-Tadano, S., Ivanovic, R., Gregoire, L., Lang, C., Gandy, N., Gregory, J., Edwards, T. L., Pollard, O., & Smith, R. S. (2024). Large-ensemble simulations of the North American and Greenland ice sheets at the Last Glacial Maximum with a coupled atmospheric general circulation–ice sheet model. *Climate of the Past*, *20*(7), 1489–1512. https://doi.org/10.5194/cp-20-1489-2024

Strzelecki, M. C., & Jaskólski, M. W. (2020). Arctic tsunamis threaten coastal landscapes and communities – survey of Karrat Isfjord 2017 tsunami effects in Nuugaatsiaq, western Greenland. *Natural Hazards and Earth System Sciences*, *20*(9), 2521–2534. https://doi.org/10.5194/nhess-20-2521-2020

Sulak, D. J., Sutherland, D. A., Enderlin, E. M., Stearns, L. A., & Hamilton, G. S. (2017). Iceberg properties and distributions in three Greenlandic fjords using satellite imagery. *Annals of Glaciology*, *58*(74), 92–106. https://doi.org/10.1017/aog.2017.5

Sutherland, D. A., Jackson, R. H., Kienholz, C., Amundson, J. M., Dryer, W. P., Duncan, D., Eidam, E. F., Motyka, R. J., & Nash, J. D. (2020). *Water temperature, salinity, currents, and others collected by conductivity, temperature and pressure (CTD) and acoustic doppler current profiler (ADCP) from MV Steller and MV Pelican in LeConte Bay, Alaska from 2016-08-09 to 2018-09-18 (NCEI Accession 0189574)* [Text/xml]. NSF Arctic Data Center. https://doi.org/10.18739/A2WW77125

Svennevig, K. (2019). Preliminary landslide mapping in Greenland. *Geological Survey of Denmark and Greenland Bulletin*, *43*. https://doi.org/10.34194/GEUSB-201943-02-07

Svennevig, K., Hicks, S. P., Forbriger, T., Lecocq, T., Widmer-Schnidrig, R., Mangeney, A., Hibert, C., Korsgaard, N. J., Lucas, A., Satriano, C., Anthony, R. E., Mordret, A., Schippkus, S., Rysgaard, S., Boone, W., Gibbons, S. J., Cook, K. L., Glimsdal, S., Løvholt, F., … Wirtz, B.

(2024). A rockslide-generated tsunami in a Greenland fjord rang Earth for 9 days. *Science*, *385*(6714), 1196–1205. https://doi.org/10.1126/science.adm9247

University Of Alaska Southeast. (2019). *LeConte Glacier time-lapse photos, LeConte Glacier, Alaska, 2018* [Dataset]. Arctic Data Center. https://doi.org/10.18739/A27W6754N

Wagner, T. J. W., Stern, A. A., Dell, R. W., & Eisenman, I. (2017). On the representation of capsizing in iceberg models. *Ocean Modelling*, *117*, 88–96. https://doi.org/10.1016/j.ocemod.2017.07.003

Wolper, J., Gao, M., Lüthi, M. P., Heller, V., Vieli, A., Jiang, C., & Gaume, J. (2021). A glacier–ocean interaction model for tsunami genesis due to iceberg calving. *Communications Earth & Environment*, *2*(1), 130. https://doi.org/10.1038/s43247-021-00179-7

Ye, Q., Wang, Y., Liu, L., Guo, L., Zhang, X., Dai, L., Zhai, L., Hu, Y., Ali, N., Ji, X., Ran, Y., Qiu, Y., Shi, L., Che, T., Wang, N., Li, X., & Zhu, L. (2024). Remote Sensing and Modeling of the Cryosphere in High Mountain Asia: A Multidisciplinary Review. *Remote Sensing*, *16*(10), 1709. https://doi.org/10.3390/rs16101709

Zemp, M., Huss, M., Thibert, E., Eckert, N., McNabb, R., Huber, J., Barandun, M., Machguth, H., Nussbaumer, S. U., Gärtner-Roer, I., Thomson, L., Paul, F., Maussion, F., Kutuzov, S., & Cogley, J. G. (2019). Global glacier mass changes and their contributions to sea-level rise from 1961 to 2016. *Nature*, *568*(7752), 382–386. https://doi.org/10.1038/s41586-019-1071-0